Search for decays of stopped exotic long-lived particles produced in proton-proton collisions at $\sqrt{s} = 13\,\text{TeV}$

The CMS collaboration

E-mail: cms-publication-committee-chair@cern.ch

ABSTRACT: A search is presented for the decays of heavy exotic long-lived particles (LLPs) that are produced in proton-proton collisions at a center-of-mass energy of 13 TeV at the CERN LHC and come to rest in the CMS detector. Their decays would be visible during periods of time well separated from proton-proton collisions. Two decay scenarios of stopped LLPs are explored: a hadronic decay detected in the calorimeter and a decay into muons detected in the muon system. The calorimeter (muon) search covers a period of sensitivity totaling $721\,(744)$ hours in $38.6\,(39.0)\,\text{fb}^{-1}$ of data collected by the CMS detector in 2015 and 2016. The results are interpreted in several scenarios that predict LLPs. Production cross section limits are set as a function of the mean proper lifetime and the mass of the LLPs, for lifetimes between 100 ns and 10 days. These are the most stringent limits to date on the mass of hadronically decaying stopped LLPs, and this is the first search at the LHC for stopped LLPs that decay to muons.

Contents

1 Introduction

Heavy long-lived particles (LLPs) on the order of 100 GeV are not present in the standard model (SM). Therefore, any sign of them would be an indication of new physics. Many extensions of the SM predict the existence of LLPs [1–8]. At the CERN LHC, the LLPs will stop inside the detector material if they lose all of their kinetic energy while traversing the detector, which will typically occur for particles with initial velocities less than about $0.5c$ [9]. This energy loss can occur via nuclear interactions if they are strongly interacting and/or through ionization if they are charged. The observation of a stopped particle decay

signature would not only indicate new physics but also help measure the lifetime of LLPs, giving insights into various beyond the standard model (BSM) theories.

If these stopped LLPs have lifetimes longer than tens of nanoseconds, most of their decays would be reconstructed as separate events unrelated to their production [10]. Owing to the difficulty of differentiating between the LLP decay products and SM particles from LHC proton-proton (pp) collisions, these subsequent decays are most easily identified when there are no proton bunches in the detector. The detector is quiet during these out-of-collision time periods with the exception of rare noncollision backgrounds, such as cosmic rays, beam halo particles, and detector noise. If LLPs come to a stop in the detector, they are most likely to do so in the densest detector materials, which in the CMS detector are the electromagnetic calorimeter (ECAL), the hadron calorimeter (HCAL), and the steel yoke in the muon system. If the stopped LLPs decay in the calorimeters, relatively large energy deposits occurring in the intervals between collisions could be observed. Furthermore, if the stopped LLPs decay into muons, displaced muon tracks out of time with the collisions could be detected.

In this paper we present two searches for stopped LLPs that decay out of time with respect to the presence of proton bunches in the detector. One search targets hadronic decays detected in the calorimeters, and the other looks for decays to muon pairs in the muon system. These two search channels are analyzed independently using data collected by the CMS experiment in 2015 and 2016 with separate dedicated triggers. The calorimeter (muon) search uses $\sqrt{s} = 13\,\text{TeV}$ data corresponding to an integrated luminosity of $38.6\,(39.0)\,\text{fb}^{-1}$ collected with LHC pp collisions separated by $25\,\text{ns}$ during a search interval totaling $721\,(744)$ hours. The size of the search sample is further reduced by applying a series of offline selection criteria to decrease the number of events that most likely come from the primary sources of background.

The calorimeter search presented here improves upon previous searches performed by the CMS collaboration, the most recent of which used $\sqrt{s} = 8\,\text{TeV}$ pp collision data corresponding to an integrated luminosity of $18.6\,\text{fb}^{-1}$ collected in 2012 [11]. This search excluded long-lived gluinos ($\widetilde{\text{g}}$) with masses below $880\,\text{GeV}$ and long-lived top squarks ($\widetilde{\text{t}}$) with masses below $470\,\text{GeV}$, for lifetimes between $10\,\mu\text{s}$ and $1000\,\text{s}$. The results of earlier, similar searches have been reported by the D0 collaboration at the Tevatron [12] and by the CMS [13, 14] and ATLAS collaborations [15, 16]. The displaced muon search is newly added to investigate different models with leptonic decays of stopped LLPs, such as those of gluinos [9] and multiply charged massive particles (MCHAMPs) [17–20]. Searches for decays of stopped LLPs are complementary to searches for heavy stable charged particles (HSCPs) that pass through the detector and can be identified by their energy loss and time-of-flight (TOF) information [21–34]. The searches presented here would allow the study of the decay of such heavy particles, whereas dedicated HSCP searches typically look for the particle itself, before it decays. However, both the searches for decays of stopped LLPs and for HSCPs are sensitive to a similar range of lifetimes.

2   The CMS detector

The central feature of the CMS apparatus is a superconducting solenoid of 6 m internal diameter, providing a magnetic field of 3.8 T. Within the solenoid volume are a silicon pixel and strip tracker, a lead tungstate crystal ECAL, and a brass and scintillator HCAL, each composed of a barrel and two endcap sections. Forward calorimeters extend the pseudorapidity η coverage provided by the barrel and endcap detectors. In the region $|\eta| < 1.74$, the HCAL cells have widths of 0.087 in η and 0.087 radians in azimuth (ϕ). In the η-ϕ plane, and for $|\eta| < 1.48$, the HCAL cells map on to 5×5 arrays of ECAL crystals to form calorimeter towers projecting radially outwards from close to the nominal pp collision interaction point (IP). For $|\eta| > 1.74$, the coverage of the towers increases progressively to a maximum of 0.174 in $\Delta\eta$ and $\Delta\phi$. Within each tower, the energy deposits in ECAL and HCAL cells are summed to define the calorimeter tower energies, which are subsequently used to provide the energies and directions of hadronic jets. In the HCAL barrel (HB) and endcap, scintillation light is detected by hybrid photodiodes (HPDs), and each HPD collects signals from 18 different HCAL channels. Signals from four HPDs are then digitized by analog-to-digital converters within a single readout box (RBX).

Muons are measured in gas-ionization chambers embedded in the steel flux-return yoke outside the solenoid. Muons are measured in the range $|\eta| < 2.4$, with detection planes made using three technologies: drift tubes (DTs) in the barrel, cathode strip chambers (CSCs) in the endcaps, and resistive plate chambers (RPCs) in both the barrel and the endcaps. All these technologies provide both position and timing information. Hits within each DT or CSC chamber are matched to form a reconstructed DT or CSC segment.

The first level (L1) of the CMS trigger system, composed of custom hardware processors, uses information from the calorimeters and muon detectors to select the most interesting events in a fixed time interval of less than 4 μs. The high-level trigger processor farm further decreases the event rate from around 100 kHz to less than 1 kHz, before data storage.

A more detailed description of the CMS detector, together with a definition of the coordinate system used and the relevant kinematic variables, can be found in ref. [35].

3   Data and Monte Carlo simulation

3.1   Data samples

The LHC accelerates two proton beams in opposite directions such that the protons collide at several points along the LHC ring, including one at the CMS detector. Each LHC beam consists of a number of proton bunches arranged into an irregular pattern of "trains" [36]. Within a train, the proton bunches are nominally spaced 25 ns apart, with a larger spacing between trains to account for the needs of the injection process. In an LHC orbit there are 3564 bunch slots (BXs), which are 25 ns long. Each BX could be filled with proton bunches, which usually occupy the first 2.5 ns of the BX, or could be empty. The trains may be spaced such that there could be multiple empty BXs between filled BXs. To search for LLP decays during these empty BXs, dedicated triggers select events at least two BXs

away from any proton bunches. Thus these triggers are live only during these specific time windows. This distance of two BXs is chosen so that we maximize the search time window while suppressing most of the events from secondary pp interactions and from "beam halo", which are mostly muons traveling outside the LHC beam that are produced by LHC beam-collimator scattering.

The search is performed with $\sqrt{s} = 13\,\text{TeV}$ pp collision run data collected by the CMS experiment in 2015 and 2016. The 2015 calorimeter (muon) search sample, taken between August and November 2015, corresponds to an integrated luminosity of $2.7\,(2.8)\,\text{fb}^{-1}$ and spans a trigger livetime, which is the amount of time the triggers are live in between collisions, of 135 (155) hours. The 2016 calorimeter (muon) search sample was taken between May and October 2016, during which a data sample corresponding to an integrated luminosity of $35.9\,(36.2)\,\text{fb}^{-1}$ was recorded, spanning a trigger livetime of 586 (589) hours. We do not consider the possibility of LLPs that were produced in 2015 but decayed in 2016. In both the 2015 and 2016 searches, we use cosmic run data collected by dedicated triggers as a control sample. These dedicated cosmic run data were recorded during LHC machine technical stops, several days after collision runs. A negligible amount of long-lived signal produced during collisions could have decayed during these cosmic runs for the lifetimes considered in this analysis. The instrumental noise background estimate is extrapolated from the instrumental noise measured in these control samples. Most of the other sources of background are estimated from sideband regions of the main data sample, except for the cosmic ray muon background in the calorimeter search, which is estimated from MC simulation.

3.2 Benchmark models

Several simplified models are considered in this search, and samples are generated for each using Monte Carlo (MC) simulation.

In the calorimeter search, we interpret the results in the context of two-body ($\widetilde{g} \rightarrow g\widetilde{\chi}^0$) and three-body ($\widetilde{g} \rightarrow q\overline{q}\widetilde{\chi}^0$) decays of a gluino into the lightest supersymmetric (SUSY) particle (LSP), the neutralino ($\widetilde{\chi}^0$). Long-lived gluinos are predicted by "split SUSY" [37, 38], in which gauginos have relatively small masses with respect to sfermions, which could be massive, since SUSY is broken at a scale much higher than the weak scale. This large mass splitting causes the long lifetime of the gluinos, since gluinos can only decay via a virtual squark. We also consider the decay of a long-lived top squark ($\widetilde{t} \rightarrow t\widetilde{\chi}^0$) that can be the next-to-LSP particle (NLSP) in various dark matter scenarios [39–41]. Here the LSP should be loosely interpreted as any new, neutral, non-interacting fermion, and not necessarily as a SUSY neutralino.

In the muon search, we consider a different model for a three-body decay of the gluino ($\widetilde{g} \rightarrow q\overline{q}\widetilde{\chi}_2^0, \widetilde{\chi}_2^0 \rightarrow \mu^+\mu^-\widetilde{\chi}^0$), which is complementary to the calorimeter search. In this model, the mass of the LSP neutralino ($\widetilde{\chi}^0$) is chosen to be 0.25 times the gluino mass, and the mass of the NLSP neutralino ($\widetilde{\chi}_2^0$) is chosen to be 2.5 times the LSP neutralino mass. A second simplified model used in the muon search predicts exotic particles called MCHAMPs, whose charges are multiples of the elementary charge e and which are predicted

by several BSM theories [20]. We assume an MCHAMP with charge $|Q| = 2e$ decays into two same-sign muons (MCHAMP $\to \mu^{\pm}\mu^{\pm}$).

3.3 Signal generation

The signal generation process is divided into three major stages. In Stage 1, the LLPs for each signal process are generated from pp collisions with PYTHIA [42, 43] and propagated through the detector with GEANT4 v9.2 [44, 45]. For the MCHAMP signal, PYTHIA v6.4 is used, while for the gluino and top squark signals, PYTHIA v8.205 is used. If the LLPs are strongly interacting, as in the case of the gluinos and top squarks, they hadronize into R-hadrons [46–48] upon production, whose interaction with the CMS detector in the simulation is described by the cloud model [49, 50]. In this model, R-hadrons are treated as SUSY particles surrounded by a cloud of loosely bound quarks and gluons. The fraction of produced R-hadrons that contain a gluino and a valence gluon is set to 10%, a convention used in previous analyses [11, 21]. However, because the R-hadrons interact an average of ten times in the calorimeter, their flavor is effectively randomized. Some fraction of these R-hadrons are sufficiently slow moving to come to a stop in the detector material. Because they are doubly charged, MCHAMPs ionize heavily and thus a significant number also stop in the detector.

In Stage 2, the parent LLP or R-hadron is constrained to decay at the stopping position defined in Stage 1. The LLP decay is simulated by a second GEANT4 step, and the decay products are propagated through the detector.

Finally, in Stage 3, a pseudo-experiment MC simulation is conducted to estimate the probability for stopped particle decays to occur in the time window between collisions when data is being collected. The Stage 3 MC simulation determines an effective integrated luminosity by using the good data-taking periods and the LHC filling scheme to calculate the fraction of stopped particle decays that occur when the trigger is live. For a given particle lifetime, the effective integrated luminosity is defined as the total integrated luminosity multiplied by the probability that the particle decays at a time when the trigger is live in between collisions. In other words, Stages 1 and 2 determine how the signal will look in the detector, and Stage 3 determines when it will occur. More details on the signal generation process are given in refs. [11, 13, 14].

4 Event selection

The calorimeter search and the muon search employ different search strategies and thus different selection criteria, which are described in turn below.

4.1 Calorimeter search

In the calorimeter search, we look for hadronic decays of LLPs in the calorimeter that produce energy deposits that could be reconstructed as at least one high-energy jet. We trigger on calorimeter jets with energy greater than $50\,\text{GeV}$ and $|\eta| < 3$ that are at least two BXs away from pp collisions.

The major background sources are cosmic rays, beam halo, and HCAL noise. Cosmic ray and beam halo muons can emit a shower of photons via bremsstrahlung, which could be reconstructed as a jet and mistaken for signal. HCAL noise [51] can give rise to spurious signals, which in the barrel could appear in one or several HPDs within a single RBX, and thus be incorrectly reconstructed as a jet. We observe that the rate of each of these background sources drops exponentially as a function of the jet energy. We thus require the events to have a leading (highest energy) calorimeter-based jet with energy greater than 70 GeV. The calorimeter-based jets are reconstructed using an anti-k_T clustering algorithm [52, 53] with a distance parameter of 0.4. To increase the sensitivity of the search, we require that the leading jet in each event is located within $|\eta| < 1.0$, where R-hadrons are more likely to stop and where there is relatively less background from beam halo.

Secondary background sources include out-of-time collisions from remnant protons between bunches, and beam-gas interactions in the detector. The rate of these secondary background events becomes negligible after we require that there are no reconstructed collision vertices in the events.

Cosmic ray muon events usually feature a large number of reconstructed DT segments and RPC hits, whereas signal events in the calorimeter search would not. We exploit this difference to distinguish signal events from cosmic ray muons. While it is possible for the hadronic shower of an R-hadron decay to pass through the first layers of the iron yoke and induce reconstructed DT segments, these DT segments are located only in the inner layers of the muon chambers ($r < 560$ cm, where r is the transverse distance to the IP) and cluster near the leading jet. On the other hand, cosmic ray muons are equally likely to leave DT segments in all layers in both the upper and lower hemispheres of the muon system, and the angle between the jet and DT segments in ϕ is more evenly distributed. As a result, we are able to substantially reduce the cosmic ray muon background contamination in the signal region by rejecting events that have at least two DT segments in the outermost barrel layer of the muon system, events that have any DT segments in the second outermost barrel layer, events that have two DT segments with a large separation in ϕ ($|\Delta\phi| > \pi/2$), events that have DT segments in the three innermost layers that are separated in ϕ from the leading jet by at least 1.0 radian, and events that have close-by RPC hits in different layers ($\Delta R = \sqrt{(\Delta\phi)^2 + (\Delta\eta)^2} < 0.2$ and $\Delta r > 0.5$ m). We make looser DT segment requirements in the outermost than in the second outermost layer because signals are very likely to coincide with standalone DT segments that are not from cosmic ray muons but particles from the pp collision. Most of these standalone DT segments from the pp collision are located in the outermost muon barrel layer. With these selection criteria, we are able to avoid incorrectly rejecting signal events, thus increasing the signal efficiency, while still rejecting most of the cosmic ray muon events.

Beam halo muons travel closely along the beam pipe, typically traversing both sides of the muon endcap systems and resulting in a few reconstructed CSC segments. Therefore, we veto events with any CSC segments having at least five reconstructed hits. As will be discussed in section 5, since signal events may include some CSC segments, requiring a minimum number of CSC hits in the veto avoids a loss of signal efficiency.

Random electronic noise in the HCAL gives rise to events in which the time response of the HCAL readout is very different from the well-defined response from particles showering

in the calorimeter. This HCAL noise creates spurious clustered energy deposits that can be reconstructed as a jet, which would contaminate the signal region and therefore should be removed. Analog signal pulses produced by the HCAL electronics are read out over ten BXs centered around the pulse maximum. The pulse shape from showering particles consists of a peak at the collision BX and an exponential decay over the subsequent BXs. Particle showers create clustered energy deposits spread over several neighboring calorimeter towers in z and ϕ, while noise produces deposits in just one or two towers, or several towers in a single HPD or RBX. In addition to the standard HCAL noise filter [51], we use a series of offline selection criteria that exploit these timing and topological characteristics to remove the HCAL noise events. These criteria are described in detail in ref. [14].

4.2 Muon search

In the muon search, we look for LLPs where the decay products include two muons. We expect the signal to look like a pair of muons originating anywhere in the detector material, but displaced from the IP. The muons would be back-to-back in the two-body MCHAMP decay, but not for the three-body gluino decay.

The primary background sources in the muon search include cosmic ray muons, beam halo, and muon detector noise. The latter two background sources are negligible after we apply the full selection.

The trigger used in the muon search selects events at least two BXs away from the pp collision time with at least one muon reconstructed in the muon system, whose transverse momentum p_T is at least 40 GeV. As in the calorimeter search, we select events offline that have no reconstructed collision vertices.

Tracks that are reconstructed using only hits in the muon system are called standalone muon tracks [54]. However, the standard standalone track reconstruction assumes that muons originate from the IP, which is inappropriate for displaced muon searches. As a result, a new muon reconstruction algorithm was developed for this analysis, which produces displaced standalone (DSA) muon tracks [55]. The DSA tracks are reconstructed using only hits in the muon detector, and they have no constraints to the IP. Thus, DSA tracks are truly using only the muon system.

We require events to have exactly one good DSA track in the upper hemisphere of the detector and exactly one good DSA track in the lower hemisphere. Both DSA tracks must have $p_T > 50$ GeV, at least three DT chambers with valid hits, and at least three valid RPC hits. To reduce the background from beam halo, the DSA tracks must also have zero valid CSC hits.

Timing information in the DTs and RPCs, indicating whether the muon is incoming toward the detector center or outgoing away from the detector center, is used to distinguish muons from a signal event from the cosmic ray muon background. Cosmic ray muons are predominantly incoming when traversing the upper hemisphere and outgoing when traversing the lower hemisphere, as they come in from above the detector and continue to move downwards. Muons from a signal event, on the other hand, would be outgoing in both hemispheres.

We place selection criteria on both the upper and lower hemisphere DSA tracks in order to obtain a good time measurement. We require at least eight independent time measurements for the TOF computation. We require that the uncertainty in the time measured at the IP for DSA tracks, assuming the muon is outgoing, is less than 5.0 ns.

Next, we ask for the time measurement to be signal-like. We require that the direction of the lower hemisphere DSA track, as determined by a least-squares fit to the timing in each DT layer where the fit is not constrained to the IP, is consistent with being in the downward direction. We define t_{DT} as the time at the point of closest approach to the IP as measured by the DTs, assuming the muon is outgoing. Since cosmic ray muons are incoming in the upper hemisphere and outgoing in the lower hemisphere, the t_{DT} of the upper hemisphere track is expected to be 40 to 50 ns earlier than that of the lower hemisphere track. As for the signal, since both muons are outgoing, they are reconstructed to have similar times as measured at the IP. Thus, we require that Δt_{DT}, which is defined as $\Delta t_{\mathrm{DT}} = t_{\mathrm{DT}}(\mathrm{upper}) - t_{\mathrm{DT}}(\mathrm{lower})$, is greater than -20 ns, which greatly reduces the cosmic ray muon background.

In addition to these DT timing variables, we use a timing measurement from the RPCs that assigns a BX to each hit. For each of the six layers of the RPCs, the hit is given a BX assignment. A typical prompt muon created at the IP has a BX assignment of 0 for each of its RPC hits. The BX assignments of cosmic ray muons are especially useful in the lower hemisphere of the detector, as the incoming cosmic ray muons will typically trigger the event and thus be assigned BX values of 0 in each RPC layer, but the outgoing cosmic ray muons are often assigned positive BX values. For example, a lower hemisphere cosmic ray muon typically has a BX assignment of 2 for each of its good RPC hits. For the signal, each RPC BX assignment for each muon is typically 0.

Given the BX assignments in each RPC layer for a muon, we can compute the average RPC hit BX assignment multiplied by 25 ns as the RPC time for a track (t_{RPC}) and use this as a discriminating variable. A typical muon from the benchmark decays has a t_{RPC} of 0 ns for both upper and lower hemisphere DSA muon tracks. On the other hand, the t_{RPC} of a cosmic ray muon is typically 25 or 50 ns in the lower hemisphere and 0 ns in the upper hemisphere. We define $\Delta t_{\mathrm{RPC}} = t_{\mathrm{RPC}}(\mathrm{upper}) - t_{\mathrm{RPC}}(\mathrm{lower})$, and we require $\Delta t_{\mathrm{RPC}} > -7.5$ ns to further select signal-like events.

Figure 1 shows Δt_{DT} (left) and Δt_{RPC} (right) for data and MC simulation. The events shown here contain good-quality DSA muon tracks, but they are dominated by the cosmic muon background; they are selected with a subset of the criteria described above. This selection is defined by the same trigger and reconstructed vertices requirements as above. Additionally, exactly one DSA track in the upper hemisphere and exactly one DSA track in the lower hemisphere are required. Looser requirements than in the full selection are placed on the DSA track p_{T} (>10 GeV), the number of DT chambers with valid hits (greater than one), and the number of valid RPC hits (greater than one). We require the same number of DT hits with good timing measurements per DSA track and number of valid CSC hits as above for this selection. None of the remaining criteria from the main selection criteria described above are used to select the events in figure 1. As can be seen in figure 1, the number of cosmic ray muon background events is greatly reduced when the
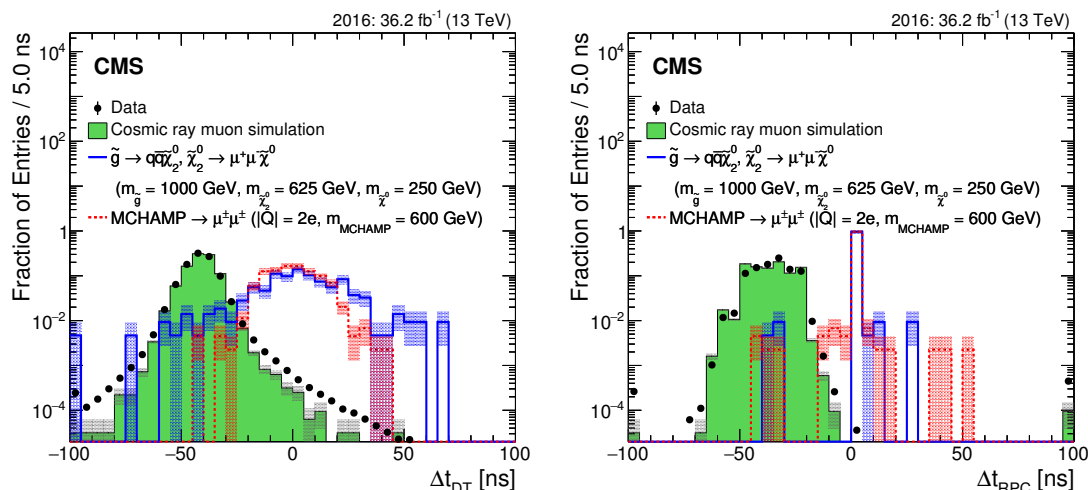
Figure 1. The Δt_{DT} (left) and Δt_{RPC} (right) distributions for 2016 data, MC simulated cosmic ray muon, 1000 GeV gluino signal, and 600 GeV MCHAMP signal events, for the muon search. The events plotted pass a subset of the full analysis selection that is designed to select good-quality DSA muon tracks but does not reject the cosmic ray muon background. The number of cosmic ray muon background events is greatly reduced when the full selection is applied, as we require $\Delta t_{\mathrm{DT}} > -20\,\mathrm{ns}$ and $\Delta t_{\mathrm{RPC}} > -7.5\,\mathrm{ns}$. The gray bands indicate the statistical uncertainty in the simulation. The histograms are normalized to unit area.

full selection is applied, as we require $\Delta t_{\mathrm{DT}} > -20\,\mathrm{ns}$ and $\Delta t_{\mathrm{RPC}} > -7.5\,\mathrm{ns}$. Since Δt_{DT} and Δt_{RPC} correspond to independent measurements of essentially the same quantity, a mismeasured cosmic ray muon is much less likely to pass both selections than just one; adding the second requirement improves the rejection of simulated cosmic ray muons by a factor of approximately 350.

5 Signal efficiency

In this section, we describe the calculation of the signal efficiency $\varepsilon_{\mathrm{signal}}$, which is the product of several efficiencies. In the calorimeter search, the stopping efficiency $\varepsilon_{\mathrm{stopping}}$ is the probability that the R-hadron stops in the HB or ECAL barrel (EB), while in the muon search, $\varepsilon_{\mathrm{stopping}}$ is the probability of each LLP to stop in any region of the detector. The Stage 1 simulation determines $\varepsilon_{\mathrm{stopping}}$. The reconstruction efficiency $\varepsilon_{\mathrm{reco}}$ is the efficiency of an event to pass all of the selection criteria, including the trigger, and it is computed independently of $\varepsilon_{\mathrm{stopping}}$. In addition, $\varepsilon_{\mathrm{reco}}$ is calculated assuming that the LLP decay occurs when the trigger is live in between collisions, and assuming a branching fraction ($\mathcal{B}$) of 100% to the decays in the signal models described above. The Stage 2 simulation determines $\varepsilon_{\mathrm{reco}}$. The efficiency $\varepsilon_{\mathrm{signal}}$ is defined as the product of $\varepsilon_{\mathrm{stopping}}$ and $\varepsilon_{\mathrm{reco}}$ for the muon search. For the calorimeter search, $\varepsilon_{\mathrm{signal}}$ is the product of $\varepsilon_{\mathrm{stopping}}$, $\varepsilon_{\mathrm{reco}}$, and two additional factors, $\varepsilon_{\mathrm{CSCveto}}$ and $\varepsilon_{\mathrm{DTveto}}$, which are defined in the next subsection.

5.1 Calorimeter search

For the calorimeter search, $\varepsilon_{\mathrm{stopping}}$ is constant at about 0.054 for gluinos and 0.045 for top squarks, for the range of masses considered. The $\varepsilon_{\mathrm{stopping}}$ value is larger for gluinos

	$\widetilde{g} \to g\widetilde{\chi}^0$	$\widetilde{g} \to q\overline{q}\widetilde{\chi}^0$	$\widetilde{t} \to t\widetilde{\chi}^0$
$\varepsilon_{\text{stopping}}$	0.054	0.054	0.045
$\varepsilon_{\text{reco}}$	0.533	0.566	0.399
$\varepsilon_{\text{CSCveto}}$	0.944	0.944	0.944
$\varepsilon_{\text{DTveto}}$	0.877	0.877	0.877
$\varepsilon_{\text{signal}}$	0.023	0.025	0.014

Table 1. Summary of the values of $\varepsilon_{\text{stopping}}$, $\varepsilon_{\text{CSCveto}}$, $\varepsilon_{\text{DTveto}}$, and the plateau value of $\varepsilon_{\text{reco}}$ for different signals, for the calorimeter search. The efficiency $\varepsilon_{\text{stopping}}$ is constant for the range of signal masses considered. The efficiency $\varepsilon_{\text{reco}}$ is given on the E_{g} or E_{t} plateau for each signal.

than for top squarks of the same mass because gluinos are more likely to produce doubly charged R-hadrons.

The value of $\varepsilon_{\text{reco}}$ depends primarily on the energy of the visible daughter particle(s) of the R-hadron decay, denoted by E_{g} (E_{t}) if the daughter is a gluon (top quark). When $E_{\text{g}} >$ 130 GeV ($E_{\text{t}} > 170$ GeV), $\varepsilon_{\text{reco}}$ becomes approximately constant, as shown in figure 2. For the three-body gluino decay, $\varepsilon_{\text{reco}}$ depends approximately on the mass difference between $\widetilde{g}$ and $\widetilde{\chi}^0$, becoming constant when $m_{\widetilde{g}} - m_{\widetilde{\chi}^0} \gtrsim 160$ GeV.

Some physical effects that are not modeled in simulation can cause reconstructed CSC or DT segments that are out of time with respect to a collision. For example, thermal neutrons can take up to a tenth of a second after being produced in pp collisions before they arrive at the muon detectors and induce a signal in the CSCs or DTs. Since these segments can occur when the trigger is live, it is possible that some of the events in the search sample could contain such segments. These events would be rejected by the selection criteria, thus decreasing the probability for a signal to be observed. The terms $\varepsilon_{\text{CSCveto}}$ and $\varepsilon_{\text{DTveto}}$ measure this decrease in efficiency due to these sources.

We define $\varepsilon_{\text{CSCveto}}$ ($\varepsilon_{\text{DTveto}}$) as the conditional probability that a signal passes the beam halo (cosmic ray muon) rejection criteria assuming the potential occurrence of coincident CSC (DT) segments, given that the signal itself passes the full selection criteria. HCAL noise events that are collected by the trigger are used to estimate these two efficiencies from data, since this noise is independent of any muon detector activities and should pass both beam halo rejection and cosmic ray muon rejection criteria. These events are selected by inverting some of the noise rejection criteria. Then $\varepsilon_{\text{CSCveto}}$ ($\varepsilon_{\text{DTveto}}$) is simply the percentage of noise events that survive the beam halo (cosmic ray muon) vetoes among all selected noise events.

Table 1 summarizes the values of $\varepsilon_{\text{stopping}}$, $\varepsilon_{\text{CSCveto}}$, $\varepsilon_{\text{DTveto}}$, and the plateau value of $\varepsilon_{\text{reco}}$.

5.2 Muon search

Tables 2 and 3 show $\varepsilon_{\text{stopping}}$ and $\varepsilon_{\text{reco}}$ for each assumed signal mass in the muon search. The $\varepsilon_{\text{signal}}$ value is the product of these two efficiencies. The $\varepsilon_{\text{stopping}}$ value is larger for MCHAMPs than for gluinos because the MCHAMPs considered have $|Q| = 2e$ and the
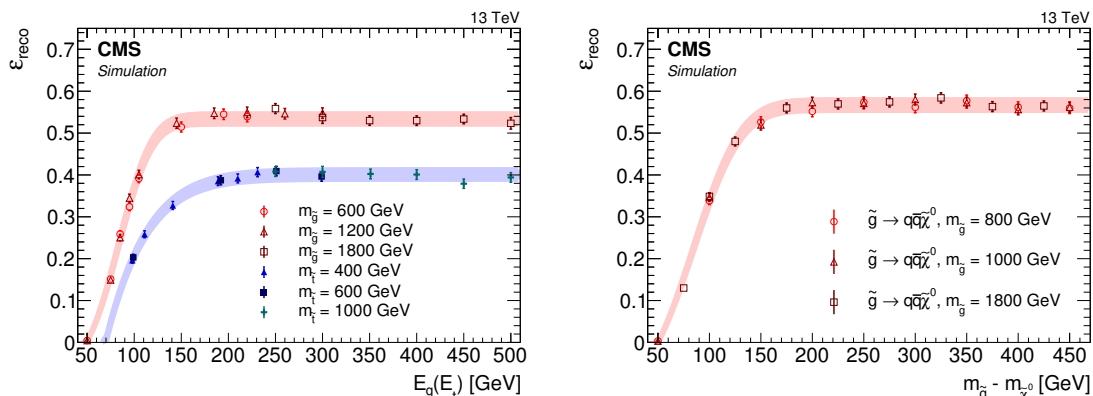
Figure 2. The $\varepsilon_{\mathrm{reco}}$ values as a function of E_{g} or E_{t} (left), and $m_{\widetilde{\mathrm{g}}} - m_{\widetilde{\chi}^0}$ (right), for $\widetilde{\mathrm{g}}$ and $\widetilde{\mathrm{t}}$ R-hadrons that stop in the EB or HB, in the MC simulation, for the calorimeter search. The $\varepsilon_{\mathrm{reco}}$ values are plotted for the two-body gluino and top squark decays (left) and for the three-body gluino decay (right). The shaded bands correspond to the systematic uncertainties, which are described in section 7.

$m_{\widetilde{\mathrm{g}}}$ [GeV]	$\varepsilon_{\mathrm{stopping}}$	$\varepsilon_{\mathrm{reco}}$	Expected events
400	0.19	0.0015	400
600	0.17	0.0024	50
800	0.17	0.0037	10
1000	0.17	0.0029	2
1200	0.18	0.0025	0.5
1400	0.20	0.0031	0.2
1600	0.21	0.0029	0.1

Table 2. Gluino $\varepsilon_{\mathrm{stopping}}$ and $\varepsilon_{\mathrm{reco}}$, as well as the number of expected gluino events with lifetimes between $10\,\mu\mathrm{s}$ and $1000\,\mathrm{s}$, assuming $\mathcal{B}(\widetilde{\mathrm{g}} \to \mathrm{q}\overline{\mathrm{q}}\widetilde{\chi}_2^0)\mathcal{B}(\widetilde{\chi}_2^0 \to \mu^+\mu^-\widetilde{\chi}^0) = 100\%$, for each mass point considered for the 2016 muon search. The efficiencies are constant for this range of lifetimes.

gluinos sometimes produce singly charged R-hadrons. We lose signal efficiency because the L1 muon trigger is designed to identify muons coming from the IP, although the muons from the signal can be very displaced. A further loss in signal efficiency is due to the very strict requirements on the quality of the DSA muon track. Similarly, the requirement to have exactly one DSA track traversing the upper hemisphere and exactly one DSA track traversing the lower hemisphere further reduces the geometrical acceptance, particularly for the gluino decay, which does not produce back-to-back muons, unlike the MCHAMP decay. The numbers in tables 2 and 3 represent the maximum number of signal events that can be measured before applying the different search windows depending on the lifetime of the stopped particle.

6 Background estimation

Since the background sources in both the calorimeter and the muon searches are not well modeled in simulation, we use control samples in data to estimate their contributions after the full event selection is applied.

m_{MCHAMP} [GeV]	$\varepsilon_{\mathrm{stopping}}$	$\varepsilon_{\mathrm{reco}}$	Expected events
100	0.33	0.0059	100
200	0.29	0.041	50
400	0.28	0.045	4
600	0.25	0.042	0.5
800	0.30	0.038	0.1

Table 3. MCHAMP $\varepsilon_{\mathrm{stopping}}$ and $\varepsilon_{\mathrm{reco}}$, as well as the number of expected MCHAMP events with lifetimes between $10\,\mu$s and $1000\,$s, assuming $\mathcal{B}(\mathrm{MCHAMP} \to \mu^{\pm}\mu^{\pm}) = 100\%$, for each mass point considered for the 2016 muon search. The efficiencies are constant for this range of lifetimes.

6.1 Calorimeter search

After applying the selection criteria in the calorimeter search, some background sources from cosmic ray muons, beam halo, and calorimeter noise remain in the data. We quantify the probability of background events escaping the background vetoes and thus being observed by this search. These inefficiencies are calculated as follows.

We generate a sample of cosmic ray muon events to estimate the rate of such events escaping the cosmic ray muon rejection criteria. The events are generated using CMSC-GEN [56], a generator based on the air shower program CORSIKA [57] and validated in a CMS analysis [58]. We require that the events pass the preselection criteria, namely that they are required to have substantial energy deposits in the calorimeter and no CSC segments in the muon endcap system. The cosmic ray muon veto inefficiency is defined as the fraction of preselected simulated cosmic ray muon events that are not rejected by the cosmic ray muon rejection criteria. It is found to be 1×10^{-3}. To account for the small difference in occupancy between the cosmic ray muon events in data and MC simulation, we first bin the simulated events in the number of DT and outer barrel RPC hits and calculate the inefficiency bin by bin. Then, we apply the halo veto and the noise veto to a sample of events in data, and bin these data events in the same way as the simulated events. For each bin, we multiply the inefficiency by the number of events in data, giving the binned cosmic ray muon prediction. The nominal cosmic ray muon background prediction is then the sum of the events in each bin.

The uncertainty in the cosmic ray muon background is due to the uncertainty in the estimate of muons that escape detection by passing through uninstrumented regions of the CMS detector, which is necessarily estimated from simulation. Since data in the uninstrumented regions are *ipso facto* not available to compare to simulation, we define equivalent fiducial volumes of instrumented regions of the muon system. Using these as a proxy for the uninstrumented regions, we assess the reliability of the simulation by comparing data and simulation. We find the average discrepancy between cosmic ray muon data and simulation in the number of detected muons traveling through various fiducial regions in the detector to be about 32%, and we assign this to be the systematic uncertainty in the cosmic ray muon background estimate. Thus, we estimate the cosmic ray muon background to be $2.6 \pm 0.9\,(8.8 \pm 3.1)$ events in 2015 (2016) data.

Because there was a high rate of beam halo production in 2015 and 2016 data, and because it is possible for halo muons to escape the acceptance of the endcap muon system, the halo background is nonnegligible. We estimate the halo veto inefficiency using a tag-and-probe method [59] that analyzes a high-purity sample of halo events by selecting events having one calorimeter jet with $|\eta| < 1.0$ and CSC segments in at least two endcap layers of the muon system. Since the rates of beam halo in each beam are not the same, the events are first classified according to whether they originated in the clockwise ($-z$ direction) or the counterclockwise ($+z$ direction) beam. Then for each class, depending on whether these events have CSC segments in only one endcap or both endcaps of the muon system, they are categorized into events that have only the incoming portion of a halo muon track, events that have only the outgoing portion, and events that have both portions. The number of events that escape detection is $N_{\text{IncomingOnly}} N_{\text{OutgoingOnly}} / N_{\text{Both}}$. We define $N_{\text{IncomingOnly}}$ ($N_{\text{OutgoingOnly}}$) as the number of events that have only an incoming (outgoing) portion of a halo muon track. The number of events that have both an incoming and an outgoing halo muon track is N_{Both}. After binning halo events in their x and y coordinates and performing the classification and calculation discussed above, we estimate the halo veto inefficiency to be 1×10^{-4}. We then multiply this inefficiency by the number of halo events vetoed in the search region.

To account for the possibility that the x-y binning does not reproduce the actual shape of the inactive or uninstrumented regions of the detector, thus biasing the estimate, we repeat the calculation above, but binning events in ϕ and r instead. The systematic uncertainty is then defined as the difference between the results from the two binning schemes. We find a halo background estimate of 1.1 ± 0.1 (2.6 ± 0.2) events in 2015 (2016) data.

Finally, the background estimation of instrumental noise is performed using control data in dedicated cosmic runs with no beams in the LHC, which include only cosmic ray muon and noise events. We select cosmic runs taken several days after pp collision runs so that there would be little chance for the signal to appear. After applying all selection criteria on the control data, we observe 2 events in each of the 2015 and 2016 control data. We then subtract the expected cosmic ray muon background from the total event yield, obtaining a noise background estimate of $0.3^{+2.4}_{-0.3}$ ($0.0^{+2.2}_{-0.0}$) events in 2015 (2016) control data. Based on the number of noise events in the control sample, we expect the noise veto inefficiency to be $\leq 1 \times 10^{-4}$. These noise estimates are then scaled to the search data, assuming that the noise veto inefficiency remains the same. The resulting noise background estimate is $0.4^{+2.9}_{-0.4}$ ($0.0^{+9.8}_{-0.0}$) events in 2015 (2016). The uncertainty in the 2016 prediction is large because the trigger livetime of the cosmic runs in 2016 was about 60% shorter than that of the collision runs, and also because the 2016 trigger livetime in collision runs is larger than the 2015 trigger livetime. Therefore, the uncertainty is scaled by a larger factor.

The total background estimate for the calorimeter search is $4.1^{+3.0}_{-1.0}$ ($11.4^{+10.3}_{-3.1}$) events in 2015 (2016), as summarized in table 4.

6.2 Muon search

In the muon search, a small number of cosmic ray muon background events remains after applying the full event selection to the data. The cosmic ray muon background is estimated

LHC period	Trigger livetime [hrs]	HCAL noise	Cosmic ray muons	Beam halo	Total background
2015	135	$0.4^{+2.9}_{-0.4}$	2.6 ± 0.9	1.1 ± 0.1	$4.1^{+3.0}_{-1.0}$ (6.2)
2016	586	$0.0^{+9.8}_{-0.0}$	8.8 ± 3.1	2.6 ± 0.2	$11.4^{+10.3}_{-3.1}$ (17.4)

Table 4. The background prediction for the calorimeter search. The total background median value is listed in parentheses; this value corresponds directly to the median expected limits shown below.

by extrapolating the data from a background-dominated region into the signal region. We apply the full event selection to the data except the $\Delta t_{\rm DT}$ criterion and invert the $\Delta t_{\rm RPC}$ criterion. We then fit the $\Delta t_{\rm DT}$ distribution with the sum of two Gaussian distributions and a Crystal Ball function [60], since $\Delta t_{\rm DT}$ is relatively Gaussian with a long asymmetrical tail. Next, we compute the integral of the fit function, for $\Delta t_{\rm DT} > -20$ ns. Then, we compute the same integral after having tightened the selection criteria on $\Delta t_{\rm RPC}$ to $-50 < \Delta t_{\rm RPC} < -7.5$ ns, then $-45 < \Delta t_{\rm RPC} < -7.5$ ns, etc. in steps of 5 ns up to $-10 < \Delta t_{\rm RPC} < -7.5$ ns. Finally, we plot each integral as a function of the lower selection on $\Delta t_{\rm RPC}$, and fit this with an error function to extrapolate to the $\Delta t_{\rm RPC} > -7.5$ ns region (see figure 3). We use an error function fit in order to make a conservative background estimate. Given this extrapolation, we predict 0.04 background events in 2015 data, with a negligible statistical uncertainty, and 0.50 ± 0.02 background events in 2016 data, where the uncertainty given is statistical only. The statistical uncertainty in the background prediction derives from the uncertainty in the error function fit parameters. We checked the background prediction method by repeating the procedure with nonoverlapping $\Delta t_{\rm RPC}$ regions and found that the numbers of background events predicted are consistent with the nominal values.

The systematic uncertainty in the background prediction is evaluated by repeating the steps above, except changing the fit of the $\Delta t_{\rm DT}$ distribution to the sum of two Gaussian distributions and a Landau function [61]. Using the error function fits to extrapolate to $\Delta t_{\rm RPC} > -7.5$ ns gives a prediction of $0.07 \pm 0.06 \, (0.10 \pm 0.01)$ background events in 2015 (2016), where the uncertainty given is statistical only. Thus, the background prediction is: $0.04 \pm 0.03 \, ({\rm syst})$ background events in 2015 data, with a negligible statistical uncertainty, and $0.50 \pm 0.02 \, ({\rm stat}) \pm 0.40 \, ({\rm syst})$ background events in 2016 data.

Despite the fact that we require exactly one upper hemisphere DSA track and exactly one lower hemisphere DSA track, there could still be some background from two coincident cosmic ray muons. This background from two coincident cosmic ray muons could occur if the upper hemisphere DSA track of one cosmic ray muon is reconstructed and if the lower hemisphere DSA track of the other is also reconstructed. We estimate this contribution from data by finding the rate of events with exactly one reconstructed DSA track in one hemisphere satisfying all of the selection criteria except for the $\Delta t_{\rm DT}$ and $\Delta t_{\rm RPC}$ criteria, and no tracks in the other hemisphere. Then, making simple assumptions about when the two coincident cosmic ray muons could occur and about the DSA track reconstruction efficiency as a function of BX, we calculate the number of accidentally coincident cosmic ray muons and find it to be negligible.
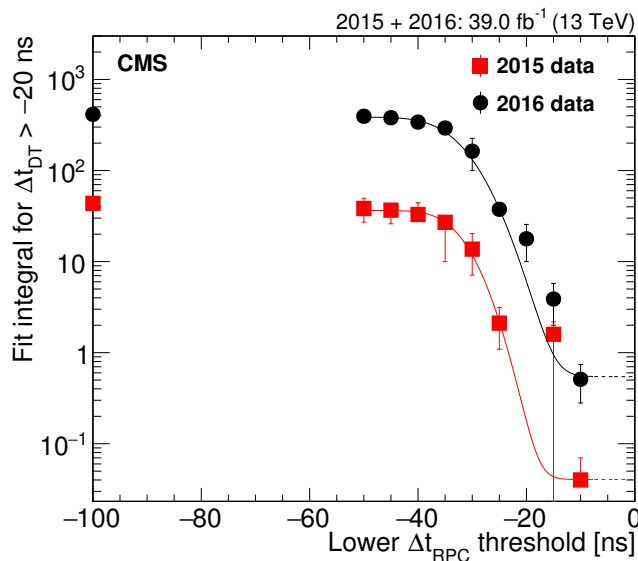
Figure 3. The background extrapolation for the muon search. The integral of the fit function to Δt_{DT} with the sum of two Gaussian distributions and a Crystal Ball function, for $\Delta t_{\mathrm{DT}} > -20$ ns, is plotted as a function of the lower Δt_{RPC} selection, for 2015 (red squares) and 2016 (black circles) data. The points are fitted with an error function and used to extrapolate to the signal region, which is defined as $\Delta t_{\mathrm{RPC}} > -7.5$ ns.

7 Systematic uncertainties in the signal efficiency

While the GEANT4 simulation used to derive the stopping probability accurately models both the electromagnetic and nuclear interaction energy loss mechanisms, the relative contributions of these energy loss mechanisms to the stopping probability depend significantly on unknown R-hadron spectroscopy. We do not consider this dependence to be a source of uncertainty for either the calorimeter or the muon search, however, since for any given model the resultant uncertainty in the stopping probability is small. Nevertheless, there are several sources of uncertainty in the signal efficiency measurement.

7.1 Calorimeter search

In the calorimeter search, the systematic uncertainty due to the trigger efficiency is negligible since the offline jet energy criterion ensures the data analyzed are well above the turn-on region, so $\varepsilon_{\mathrm{reco}}$ is constant. We consider possible systematic uncertainties in $\varepsilon_{\mathrm{CSCveto}}$ and $\varepsilon_{\mathrm{DTveto}}$ by varying the criteria used to select HCAL noise events that were described in section 5.1. We compare the efficiency of data events to pass these new HCAL noise criteria with that of the nominal HCAL noise selection criteria, and we find that the relative change in the efficiencies is less than 0.2% for both $\varepsilon_{\mathrm{CSCveto}}$ and $\varepsilon_{\mathrm{DTveto}}$, and therefore negligible. The uncertainty in the integrated luminosity is estimated as 2.3 (2.5)% for 2015 (2016) data [62, 63]. The relative uncertainty in $\varepsilon_{\mathrm{reco}}$ is estimated to be 7.7 (5.2)% for $\widetilde{\mathrm{g}}\,(\widetilde{\mathrm{t}})$ in the 2015 analysis, and 7.5 (5.2)% for $\widetilde{\mathrm{g}}\,(\widetilde{\mathrm{t}})$ in the 2016 analysis. This uncertainty, which is shown by the shaded bands in figure 2, is determined by computing the maximal relative difference among points on the plateau.

Systematic uncertainty	2015	2016
Reconstruction efficiency	7.7%	7.5%
Integrated luminosity	2.3%	2.5%
Jet energy scale	2.0%	2.0%

Table 5. Systematic uncertainties in the signal efficiency in the 2015 and 2016 calorimeter searches.

Jets in this analysis are not formed by particles originating from the center of the detector, so the standard uncertainty in the jet energy scale does not apply. Instead, we refer to a study performed on the HCAL during cosmic data taking in 2008 [64]. This study compares the energy of the reconstructed jets in simulated cosmic ray muon events and cosmic ray muon events in data, concluding that the uncertainty in the jet energy in the simulation is about 2%. Moreover, a study conducted with 2012 data [65] compares the data and simulation for dijets originating from the interaction point. The comparison leads to an estimate of <2% for jets striking the HCAL barrel with angles of incidence from 0 to $\pi/3$. After rescaling the jet energy by 2%, the signal efficiency varies by 2%. This estimate is conservative since only the yield of signals with jet energy near the offline threshold is affected by the variation of the jet energy, and as a result the uncertainty decreases rapidly as E_{g} (E_{t}) increases.

We have also considered the uncertainty associated with the jet energy resolution. Studies have shown that the signal yield is insensitive to variations in this uncertainty, and thus that the systematic uncertainty associated with the jet energy resolution is negligible.

The total systematic uncertainty in the signal yield is $8.3\,(8.2)\%$ in the 2015 (2016) search. The systematic uncertainties are summarized in table 5.

7.2 Muon search

The muon search also has several sources of systematic uncertainties. We consider the systematic uncertainty associated with the MC simulation modeling of the charge divided by the p_{T} (Q/p_{T}) resolution by comparing this resolution in cosmic ray muon data and cosmic ray muon MC simulation. The resolution compares Q/p_{T} of the upper and lower hemisphere tracks:

$$R(Q/p_{\mathrm{T}}) = \frac{(Q/p_{\mathrm{T}})^{\mathrm{upper}} - (Q/p_{\mathrm{T}})^{\mathrm{lower}}}{\sqrt{2}(Q/p_{\mathrm{T}})^{\mathrm{lower}}}.$$

We plot the standard deviation of Gaussian fits of the resolution, as a function of the lower hemisphere track p_{T}, for both cosmic ray muon data and MC simulation. A fit of the ratio between data and MC simulation in this plot for muon tracks in the lower hemisphere with $p_{\mathrm{T}} > 50\,\mathrm{GeV}$ gives a difference between cosmic ray muon data and simulation of $9.0\,(5.3)\%$ in the 2015 (2016) analysis. We propagate this resolution uncertainty to an uncertainty in the signal efficiency by smearing the momentum distribution of muons in the signal and observing the corresponding variation in the signal yields. We take the largest variation in the signal yield, namely, $13\,(7.0)\%$ in the 2015 (2016) analysis, as the systematic uncertainty in the modeling of the Q/p_{T} resolution.

Systematic uncertainty	2015	2016
Q/p_T resolution mismodeling	13%	7.0%
Trigger acceptance	13%	2.8%
Integrated luminosity	2.3%	2.5%

Table 6. Systematic uncertainties in the signal efficiency for the 2015 and 2016 muon searches.

There is also a systematic uncertainty associated with the trigger acceptance. Since the largest difference between data and MC simulation in the plateau of the trigger turn-on curves is $13\,(2.8)\%$ in the $2015\,(2016)$ analysis, we take these values as the systematic uncertainty in the trigger acceptance.

The total systematic uncertainty in the signal yield is $19\,(7.9)\%$ in the $2015\,(2016)$ search. The systematic uncertainties are summarized in table 6.

8 Results

In the calorimeter search, we predict $4.1^{+3.0}_{-1.0}$ ($11.4^{+10.3}_{-3.1}$) background events in the 2015 (2016) data. Four events that pass all of the selection criteria are observed in 2015 data, while 13 events are observed in 2016 data. Both observed numbers of events are consistent with the predicted backgrounds. The observed events are most likely cosmic ray muon or beam halo events, as they each consist of a single reconstructed jet.

In the muon search, we predict $0.04 \pm 0.03\,(0.50 \pm 0.40)$ background events in 2015 (2016). There are zero observed events in both 2015 and 2016 data that pass all of the selection criteria.

In both the calorimeter and muon searches, we count the number of observed events in equally spaced $\log_{10}$ (time) bins of signal lifetime hypotheses from 10^{-7} to 10^6 s. For lifetime hypotheses shorter than one LHC orbit of $89\,\mu$s, we search within a sensitivity-optimized time window of 1.3 times the stopped particle's lifetime, where the window starts after each pp collision, to avoid the addition of backgrounds for time intervals during which a signal with a given lifetime has a large probability to have already decayed. We assume that the cosmic ray muon background (and noise background in the calorimeter search) is uniformly distributed in time. In the calorimeter search, we estimate the halo background for each lifetime hypothesis by finding the ratio of halo events in the search time window to the total number of halo events, then multiplying this ratio by the halo background estimate for the full trigger livetime. We select the halo events by requiring events to pass all of the selection criteria except the CSC segment veto described above, and then requiring the events to have at least one CSC segment. Then, we determine if these halo events are within the search window by observing how long after the most recent filled BX they occurred.

For lifetimes longer than one orbit, the trigger livetime, the expected background, and the number of observed events are independent of the lifetime. The effective integrated luminosity decreases with lifetime for lifetimes longer than one LHC orbit, and the analysis

Lifetime [s]	Effective integrated luminosity [fb^{-1}]	Trigger livetime [hrs]	Expected background	Observed events
5×10^{-8}	0.27	17	$0.4^{+0.3}_{-0.1}$	0
8×10^{-8}	0.65	34	$0.8^{+0.6}_{-0.2}$	0
10^{-7}	1.27	67	$1.4^{+1.2}_{-0.4}$	0
10^{-6}	9.98	417	$8.4^{+7.5}_{-2.3}$	8
10^{-5}	13.37	583	$11.3^{+10.2}_{-3.1}$	13
10^{-4}	13.70	583	$11.4^{+10.3}_{-3.1}$	13
10^{3}	13.57	583	$11.4^{+10.3}_{-3.1}$	13
10^{4}	11.78	583	$11.4^{+10.3}_{-3.1}$	13
10^{5}	8.27	583	$11.4^{+10.3}_{-3.1}$	13
10^{6}	5.61	583	$11.4^{+10.3}_{-3.1}$	13

Table 7. Counting experiment results for different lifetimes in the calorimeter search with 2016 data.

sensitivity degrades with lifetimes longer than one LHC fill because any signal that decays between fills will have few chances to be observed.

For lifetime hypotheses shorter than one orbit, both the number of observed events and the expected background depend on the time window considered, which is a fraction of the total trigger livetime. Similarly, the effective integrated luminosity is reduced for short lifetimes. As we gradually increase the lifetime in the hypothesis from the minimal value, we include more observed events in the search window. When the lifetime is shorter than one orbit, to explicitly show the discontinuous changes of the upper limits whenever the expanding search window covers a new observed event, we test two lifetime hypotheses in addition to the equally spaced $\log_{10}$ (time) ones, for each observed event in these counting experiments. These two additional lifetime hypotheses are the largest lifetime hypothesis for which the event lies outside the time window, and the smallest lifetime hypothesis for which the event is contained within the time window.

Tables 7 and 8 show the results of the counting experiment for the 2016 data. The data show no excess over background, and we set upper limits on the signal production cross section (σ) using a hybrid method with the CL$_s$ criterion [66, 67] to incorporate the systematic uncertainties [68], in both the calorimeter and muon searches. By combining the likelihoods of the search results from the 2015 and 2016 analyses, we set combined upper limits on $\mathcal{B}\sigma$ for the benchmark signal models.

In the calorimeter search, the 95% confidence level (CL) upper limits on $\mathcal{B}\sigma$ for $\widetilde{g}$ ($\widetilde{t}$) pair production for combined 2015 and 2016 data as a function of the particle's lifetime τ are shown in figure 4, assuming $E_g > 130\,\text{GeV}$ ($m_{\widetilde{g}} - m_{\widetilde{\chi}^0} \gtrsim 160\,\text{GeV}$ or $E_t > 170\,\text{GeV}$). In figure 5, the gluino and top squark mass limits are shown, assuming $\mathcal{B}(\widetilde{g} \to g\widetilde{\chi}^0) = \mathcal{B}(\widetilde{g} \to q\overline{q}\widetilde{\chi}^0) = \mathcal{B}(\widetilde{t} \to t\widetilde{\chi}^0) = 100\%$. We exclude gluinos with $m_{\widetilde{g}} < 1385\,(1393)\,\text{GeV}$ that decay via $\widetilde{g} \to g\widetilde{\chi}^0$ ($\widetilde{g} \to q\overline{q}\widetilde{\chi}^0$) and top squarks with $m_{\widetilde{t}} < 744\,\text{GeV}$ at 95% CL for $10\,\mu\text{s} < \tau < 1000\,\text{s}$.

Lifetime [s]	Effective integrated luminosity [fb^{-1}]	Trigger livetime [hrs]	Expected background	Observed events
5×10^{-8}	0.27	11	0.01 ± 0.01	0
8×10^{-8}	0.64	34	0.03 ± 0.02	0
10^{-7}	1.27	68	0.06 ± 0.05	0
10^{-6}	9.95	422	0.36 ± 0.29	0
10^{-5}	13.34	581	0.49 ± 0.39	0
10^{-4}	13.67	589	0.50 ± 0.40	0
1	13.67	589	0.50 ± 0.40	0
10^{3}	13.55	589	0.50 ± 0.40	0
10^{4}	11.75	589	0.50 ± 0.40	0
10^{5}	8.26	589	0.50 ± 0.40	0
10^{6}	5.61	589	0.50 ± 0.40	0

Table 8. Counting experiment results for different lifetimes in the muon search with 2016 data.
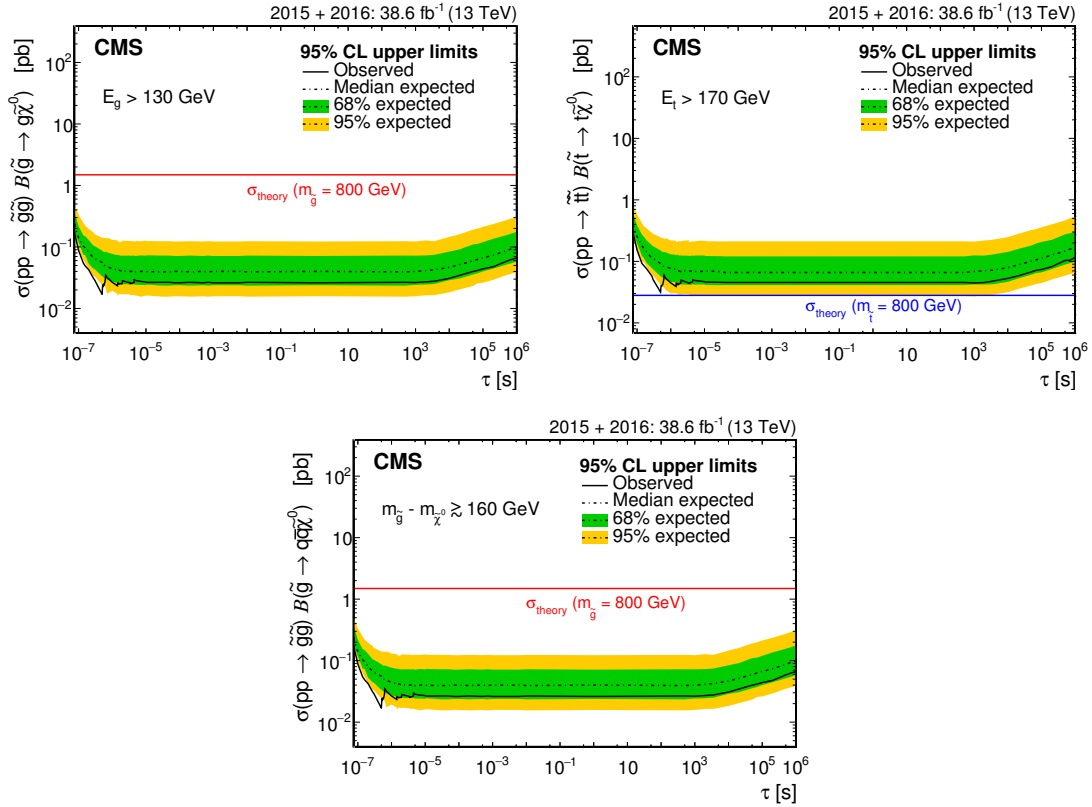
Figure 4. The 95% CL upper limits on $\mathcal{B}\sigma$ for gluino and top squark pair production, using the cloud model of R-hadron interactions, as a function of lifetime, for combined 2015 and 2016 data for the calorimeter search. We show gluinos that undergo a two-body decay (upper left), top squarks that undergo a two-body decay (upper right), and gluinos that undergo a three-body decay (lower). The discontinuous structure observed between 10^{-7} and 10^{-5} s is due to the increase of the number of observed events in the search window as the lifetime increases. The theory lines assume $\mathcal{B} = 100\%$.
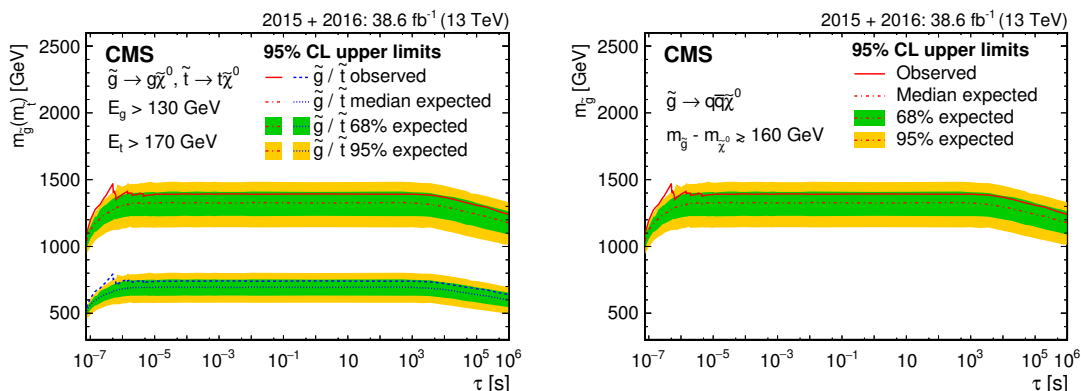
Figure 5. The 95% CL upper limits on the gluino and top squark mass, using the cloud model of R-hadron interactions, as a function of lifetime, for combined 2015 and 2016 data for the calorimeter search. We show gluinos and top squarks that undergo a two-body decay (left) and gluinos that undergo a three-body decay (right). The discontinuous structure observed between 10^{-7} and 10^{-5} s is due to the increase of the number of observed events in the search window as the lifetime increases.

Figure 6 shows the regions of the gluino (top squark) mass vs. neutralino mass plane excluded by the calorimeter search, for lifetimes between $10\,\mu$s and 1000 s. The borders of the regions are determined by the edge of the plateau in figure 2 and the gluino (top squark) mass limits.

For the muon search, the 95% CL upper limits on $\mathcal{B}\sigma$ as a function of lifetime for $1000\,$GeV gluinos and $400\,$GeV MCHAMPs are shown in figure 7 for combined 2015 and 2016 data. The combined 2015 and 2016 95% CL upper limits on $\mathcal{B}\sigma$ of gluino and MCHAMP pair production as a function of mass are shown in figure 8, for lifetimes between $10\,\mu$s and 1000 s. Gluinos with masses between 400 and $980\,$GeV are excluded for lifetimes between $10\,\mu$s and 1000 s, assuming $\mathcal{B}(\widetilde{g} \to q\overline{q}\widetilde{\chi}_2^0)\mathcal{B}(\widetilde{\chi}_2^0 \to \mu^+\mu^-\widetilde{\chi}^0) = 100\%$, $m_{\widetilde{\chi}^0} = 0.25 m_{\widetilde{g}}$ and $m_{\widetilde{\chi}_2^0} = 2.5 m_{\widetilde{\chi}^0}$. MCHAMPs with masses between 100 and $440\,$GeV and $|Q| = 2e$ are excluded for lifetimes between $10\,\mu$s and 1000 s, assuming $\mathcal{B}(\text{MCHAMP} \to \mu^\pm\mu^\pm) = 100\%$.

9 Summary

A search has been presented for long-lived particles that stopped in the CMS detector after being produced in proton-proton collisions at a center-of-mass energy of 13 TeV at the CERN LHC. The subsequent decays of these particles to produce calorimeter deposits or muon pairs were looked for during gaps between proton bunches in the LHC beams. In the calorimeter (muon) search, with collision data corresponding to an integrated luminosity of $2.7\,(2.8)\,\text{fb}^{-1}$ in a period of sensitivity corresponding to $135\,(155)$ hours of trigger livetime in 2015 and to an integrated luminosity of $35.9\,(36.2)\,\text{fb}^{-1}$ in a period of sensitivity of $586\,(589)$ hours of trigger livetime in 2016, no excess above the estimated background has been observed. Cross section (σ) and mass limits have been presented at 95% confidence level (CL) on gluino ($\widetilde{g}$), top squark ($\widetilde{t}$), and multiply charged massive particle (MCHAMP) production over 13 orders of magnitude in the mean proper lifetime of the stopped particle.
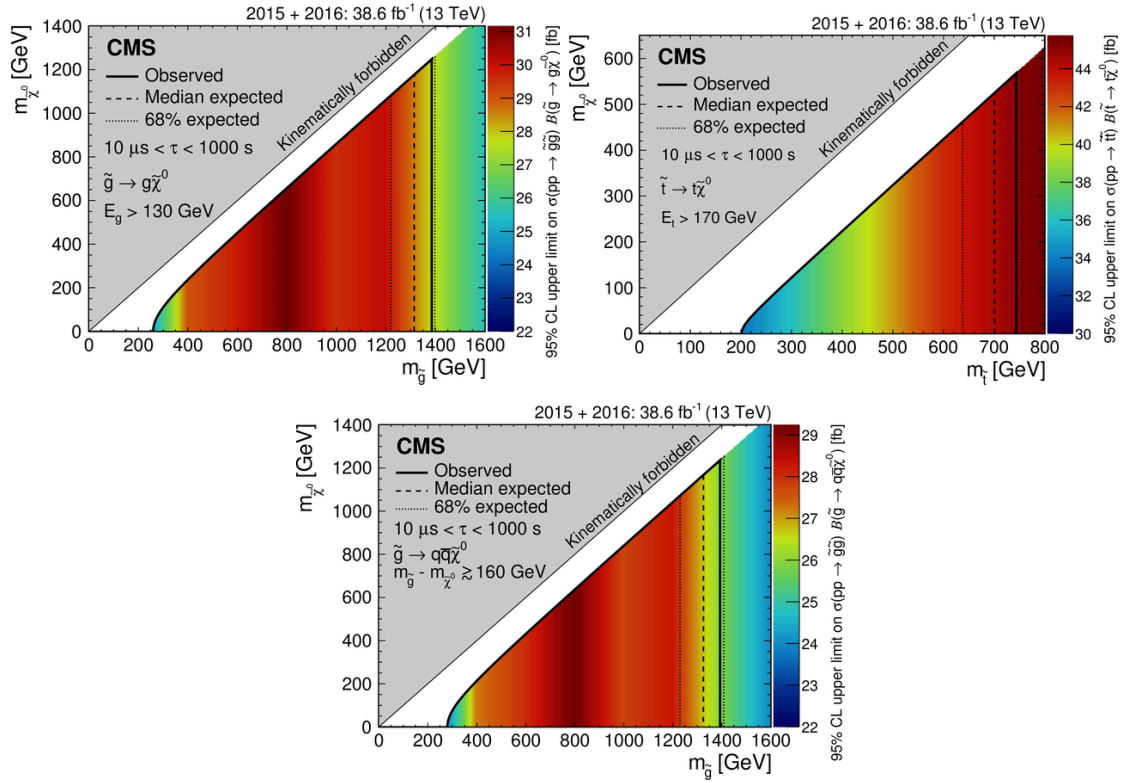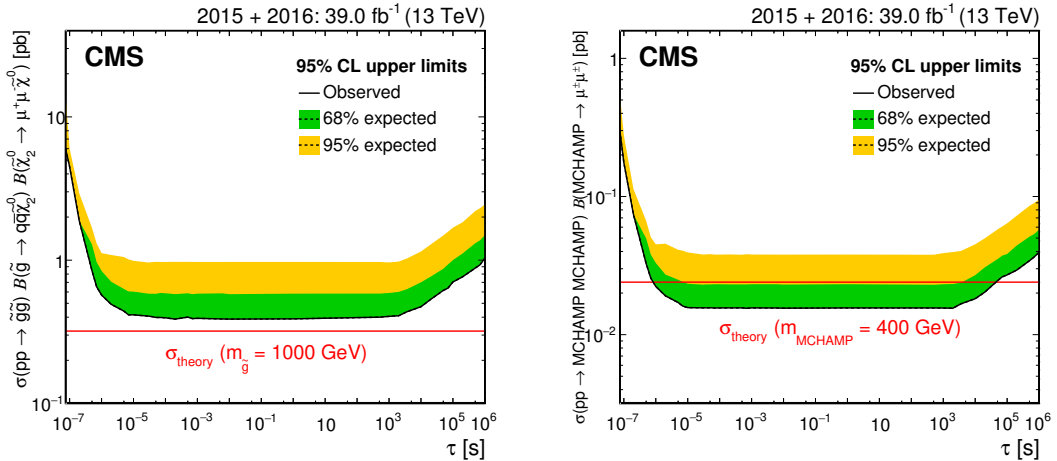
Figure 6. The 95% CL upper limits in the neutralino mass vs. gluino (top squark) mass plane, for lifetimes between $10\,\mu$s and $1000\,$s, for combined 2015 and 2016 data for the calorimeter search. The color map indicates the 95% CL upper limits on $\mathcal{B}\sigma$. The mostly triangular region defined by the black solid (dashed) line shows the excluded observed (expected) region. We show gluinos that undergo a two-body decay (upper left), top squarks that undergo a two-body decay (upper right), and gluinos that undergo a three-body decay (lower).

Figure 7. The 95% CL upper limits on $\mathcal{B}\sigma$ for $1000\,$GeV gluino (left) and $400\,$GeV MCHAMP (right) pair production as a function of lifetime, for combined 2015 and 2016 data for the muon search. The theory lines assume $\mathcal{B} = 100\%$.
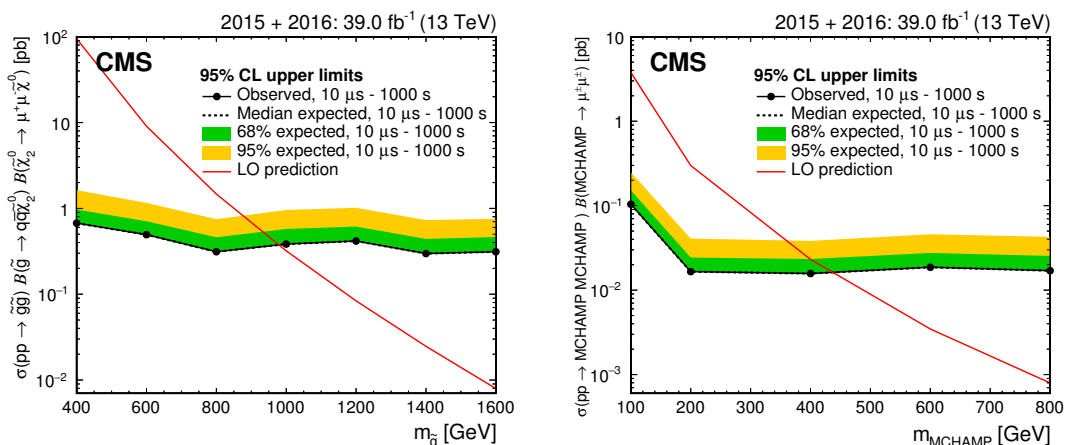
Figure 8. 95% CL upper limits on $\mathcal{B}\sigma$ for gluino (left) and MCHAMP (right) pair production as a function of mass, for lifetimes between $10\,\mu$s and $1000\,$s, for combined 2015 and 2016 data for the muon search. The theory curves assume $\mathcal{B} = 100\%$.

In the calorimeter search, combining the results from the 2015 and 2016 analyses and assuming a branching fraction ($\mathcal{B}$) of 100% for $\widetilde{g} \to g\widetilde{\chi}^0$ ($\widetilde{g} \to q\overline{q}\widetilde{\chi}^0$), where $\widetilde{\chi}^0$ is the lightest neutralino, gluinos with lifetimes from $10\,\mu$s to $1000\,$s and $m_{\widetilde{g}} < 1385\,(1393)\,$GeV have been excluded, for a cloud model of R-hadron interactions and for the daughter gluon energy $E_g > 130\,$GeV ($m_{\widetilde{g}} - m_{\widetilde{\chi}^0} \gtrsim 160\,$GeV). Under similar assumptions, for the daughter top quark energy $E_t > 170\,$GeV and $\mathcal{B}(\widetilde{t} \to t\widetilde{\chi}^0) = 100\%$, long-lived top squarks with lifetimes from $10\,\mu$s to $1000\,$s and $m_{\widetilde{t}} < 744\,$GeV have been excluded. These are the first limits on stopped long-lived particles at $13\,$TeV and the strongest limits to date.

In the muon search, 95% CL upper limits on $\mathcal{B}\sigma$ were set for combined 2015 and 2016 data. For lifetimes between $10\,\mu$s and $1000\,$s, limits were set between 1 and $0.01\,$pb for gluinos with masses between 400 and $1600\,$GeV and for MCHAMPs with masses between 100 and $800\,$GeV and charge $|Q| = 2e$. For lifetimes between $10\,\mu$s and $1000\,$s, gluinos with masses between 400 and $980\,$GeV have been excluded, assuming $\mathcal{B}(\widetilde{g} \to q\overline{q}\widetilde{\chi}_2^0)\mathcal{B}(\widetilde{\chi}_2^0 \to \mu^+\mu^-\widetilde{\chi}^0) = 100\%$, $m_{\widetilde{\chi}^0} = 0.25m_{\widetilde{g}}$, and $m_{\widetilde{\chi}_2^0} = 2.5m_{\widetilde{\chi}^0}$, where $\widetilde{\chi}_2^0$ is the next-to-lightest neutralino. Under the same lifetime hypothesis, MCHAMPs with masses between 100 and $440\,$GeV and $|Q| = 2e$ have been excluded, assuming $\mathcal{B}(\text{MCHAMP} \to \mu^{\pm}\mu^{\pm}) = 100\%$. These are the first limits obtained at the LHC for stopped particles that decay to muons.

Acknowledgments

References

[1] S. Dimopoulos, M. Dine, S. Raby and S.D. Thomas, *Experimental signatures of low-energy gauge mediated supersymmetry breaking*, *Phys. Rev. Lett.* **76** (1996) 3494 [hep-ph/9601367] [INSPIRE].

[2] H. Baer, K.-m. Cheung and J.F. Gunion, *A heavy gluino as the lightest supersymmetric particle*, *Phys. Rev.* **D 59** (1999) 075002 [hep-ph/9806361] [INSPIRE].

[3] T. Jittoh, J. Sato, T. Shimomura and M. Yamanaka, *Long life stau in the minimal supersymmetric standard model*, *Phys. Rev.* **D 73** (2006) 055009 [hep-ph/0512197] [INSPIRE].

[4] M. Fairbairn et al., *Stable massive particles at colliders*, *Phys. Rept.* **438** (2007) 1 [hep-ph/0611040] [INSPIRE].

[5] M.J. Strassler and K.M. Zurek, *Echoes of a hidden valley at hadron colliders*, *Phys. Lett.* **B 651** (2007) 374 [hep-ph/0604261] [INSPIRE].

[6] A. Arvanitaki et al., *Astrophysical Probes of Unification*, *Phys. Rev.* **D 79** (2009) 105022 [arXiv:0812.2075] [INSPIRE].

[7] N. Arkani-Hamed and S. Dimopoulos, *Supersymmetric unification without low energy supersymmetry and signatures for fine-tuning at the LHC*, *JHEP* **06** (2005) 073 [hep-th/0405159] [INSPIRE].

[8] A. Arvanitaki, N. Craig, S. Dimopoulos and G. Villadoro, *Mini-split*, *JHEP* **02** (2013) 126 [arXiv:1210.0555] [INSPIRE].

[9] A. Arvanitaki et al., *Stopping gluinos*, *Phys. Rev.* **D 76** (2007) 055007 [hep-ph/0506242] [INSPIRE].

[10] P.W. Graham, K. Howe, S. Rajendran and D. Stolarski, *New measurements with stopped particles at the LHC*, *Phys. Rev.* **D 86** (2012) 034020 [arXiv:1111.4176] [INSPIRE].

[11] CMS collaboration, *Search for decays of stopped long-lived particles produced in proton–proton collisions at $\sqrt{s} = 8\,TeV$*, *Eur. Phys. J.* **C 75** (2015) 151 [arXiv:1501.05603] [INSPIRE].

[12] D0 collaboration, V.M. Abazov et al., *Search for stopped gluinos from $p\bar{p}$ collisions at $\sqrt{s} = 1.96\,TeV$*, *Phys. Rev. Lett.* **99** (2007) 131801 [arXiv:0705.0306] [INSPIRE].

[13] CMS collaboration, *Search for stopped long-lived particles produced in pp collisions at $\sqrt{s} = 7\,TeV$*, *JHEP* **08** (2012) 026 [arXiv:1207.0106] [INSPIRE].

[14] CMS collaboration, *Search for stopped gluinos in pp collisions at $\sqrt{s} = 7\,TeV$*, *Phys. Rev. Lett.* **106** (2011) 011801 [arXiv:1011.5861] [INSPIRE].

[15] ATLAS collaboration, *Search for decays of stopped, long-lived particles from 7 TeV pp collisions with the ATLAS detector*, *Eur. Phys. J.* **C 72** (2012) 1965 [arXiv:1201.5595] [INSPIRE].

[16] ATLAS collaboration, *Search for long-lived stopped R-hadrons decaying out-of-time with pp collisions using the ATLAS detector*, *Phys. Rev.* **D 88** (2013) 112003 [arXiv:1310.6584] [INSPIRE].

[17] M. Khlopov, C.A. Stephan and D. Fargion, *Dark matter with invisible light from heavy double charged leptons of almost-commutative geometry?*, *Class. Quant. Grav.* **23** (2006) 7305 [astro-ph/0511789].

[18] A. De Rujula, S.L. Glashow and U. Sarid, *Charged dark matter*, *Nucl. Phys.* **B 333** (1990) 173 [INSPIRE].

[19] S. Dimopoulos, D. Eichler, R. Esmailzadeh and G.D. Starkman, *Getting a charge out of dark matter*, *Phys. Rev.* **D 41** (1990) 2388 [INSPIRE].

[20] P. Langacker and G. Steigman, *Requiem for an FCHAMP? Fractionally CHArged, Massive Particle*, *Phys. Rev.* **D 84** (2011) 065040 [arXiv:1107.3131] [INSPIRE].

[21] ATLAS collaboration, *Search for heavy long-lived charged particles with the ATLAS detector in pp collisions at $\sqrt{s} = 7$ TeV*, *Phys. Lett.* **B 703** (2011) 428 [arXiv:1106.4495] [InSPIRE].

[22] ATLAS collaboration, *Search for stable hadronising squarks and gluinos with the ATLAS experiment at the LHC*, *Phys. Lett.* **B 701** (2011) 1 [arXiv:1103.1984] [InSPIRE].

[23] ATLAS collaboration, *Search for massive long-lived highly ionising particles with the ATLAS detector at the LHC*, *Phys. Lett.* **B 698** (2011) 353 [arXiv:1102.0459] [InSPIRE].

[24] ATLAS collaboration, *Searches for heavy long-lived sleptons and R-Hadrons with the ATLAS detector in pp collisions at $\sqrt{s} = 7$ TeV*, *Phys. Lett.* **B 720** (2013) 277 [arXiv:1211.1597] [InSPIRE].

[25] ATLAS collaboration, *Search for long-lived, multi-charged particles in pp collisions at $\sqrt{s} = 7$ TeV using the ATLAS detector*, *Phys. Lett.* **B 722** (2013) 305 [arXiv:1301.5272] [InSPIRE].

[26] ATLAS collaboration, *Search for heavy long-lived multi-charged particles in pp collisions at $\sqrt{s} = 8$ TeV using the ATLAS detector*, *Eur. Phys. J.* **C 75** (2015) 362 [arXiv:1504.04188] [InSPIRE].

[27] ATLAS collaboration, *Search for metastable heavy charged particles with large ionisation energy loss in pp collisions at $\sqrt{s} = 8$ TeV using the ATLAS experiment*, *Eur. Phys. J.* **C 75** (2015) 407 [arXiv:1506.05332] [InSPIRE].

[28] CMS collaboration, *Searches for long-lived charged particles in pp collisions at $\sqrt{s} = 7$ and 8 TeV*, *JHEP* **07** (2013) 122 [arXiv:1305.0491] [InSPIRE].

[29] CMS collaboration, *Search for heavy stable charged particles in pp collisions at $\sqrt{s} = 7$ TeV*, *JHEP* **03** (2011) 024 [arXiv:1101.1645] [InSPIRE].

[30] CMS collaboration, *Search for fractionally charged particles in pp collisions at $\sqrt{s} = 7$ TeV*, *Phys. Rev.* **D 87** (2013) 092008 [arXiv:1210.2311] [InSPIRE].

[31] CMS collaboration, *Search for heavy long-lived charged particles in pp collisions at $\sqrt{s} = 7$ TeV*, *Phys. Lett.* **B 713** (2012) 408 [arXiv:1205.0272] [InSPIRE].

[32] CMS collaboration, *Constraints on the pMSSM, AMSB model and on other models from the search for long-lived charged particles in proton-proton collisions at $\sqrt{s} = 8$ TeV*, *Eur. Phys. J.* **C 75** (2015) 325 [arXiv:1502.02522] [InSPIRE].

[33] LHCb collaboration, *Search for long-lived heavy charged particles using a ring imaging Cherenkov technique at LHCb*, *Eur. Phys. J.* **C 75** (2015) 595 [arXiv:1506.09173] [InSPIRE].

[34] CMS collaboration, *Search for long-lived charged particles in proton-proton collisions at $\sqrt{s} = 13$ TeV*, *Phys. Rev.* **D 94** (2016) 112004 [arXiv:1609.08382] [InSPIRE].

[35] CMS collaboration, *The CMS experiment at the CERN LHC*, 2008 *JINST* **3** S08004 [InSPIRE].

[36] R. Bailey and P. Collier, *Standard filling schemes for various LHC operation modes*, LHC-PROJECT-NOTE-323 (2003).

[37] G.F. Giudice and A. Romanino, *Split supersymmetry*, *Nucl. Phys.* **B 699** (2004) 65 [*Erratum ibid.* **B 706** (2005) 487] [hep-ph/0406088] [InSPIRE].

[38] N. Arkani-Hamed, S. Dimopoulos, G.F. Giudice and A. Romanino, *Aspects of split supersymmetry*, *Nucl. Phys.* **B 709** (2005) 3 [hep-ph/0409232] [InSPIRE].

[39] D. Abercrombie et al., *Dark matter benchmark models for early LHC run-2 searches: report of the ATLAS/CMS dark matter forum*, arXiv:1507.00966 [INSPIRE].

[40] L.M. Carpenter, R. Colburn, J. Goodman and T. Linden, *Indirect detection constraints on s and t channel simplified models of dark matter*, *Phys. Rev.* **D 94** (2016) 055027 [arXiv:1606.04138] [INSPIRE].

[41] L. Covi and F. Dradi, *Long-lived stop at the LHC with or without R-parity*, *JCAP* **10** (2014) 039 [arXiv:1403.4923] [INSPIRE].

[42] T. Sjöstrand, S. Mrenna and P.Z. Skands, *PYTHIA 6.4 physics and manual*, *JHEP* **05** (2006) 026 [hep-ph/0603175] [INSPIRE].

[43] T. Sjöstrand, S. Mrenna and P.Z. Skands, *A brief introduction to PYTHIA 8.1*, *Comput. Phys. Commun.* **178** (2008) 852 [arXiv:0710.3820] [INSPIRE].

[44] GEANT4 collaboration, S. Agostinelli et al., *GEANT4 — a simulation toolkit*, *Nucl. Instrum. Meth.* **A 506** (2003) 250 [INSPIRE].

[45] J. Allison et al., *GEANT4 developments and applications*, *IEEE Trans. Nucl. Sci.* **53** (2006) 270.

[46] P. Fayet, *Spontaneously broken supersymmetric theories of weak, electromagnetic and strong interactions*, *Phys. Lett.* **69B** (1977) 489 [INSPIRE].

[47] P. Fayet, *Massive gluinos*, *Phys. Lett.* **78B** (1978) 417 [INSPIRE].

[48] G.R. Farrar and P. Fayet, *Phenomenology of the production, decay and detection of new hadronic states associated with supersymmetry*, *Phys. Lett.* **76B** (1978) 575 [INSPIRE].

[49] A.C. Kraan, *Interactions of heavy stable hadronizing particles*, *Eur. Phys. J.* **C 37** (2004) 91 [hep-ex/0404001] [INSPIRE].

[50] R. Mackeprang and A. Rizzi, *Interactions of coloured heavy stable particles in matter*, *Eur. Phys. J.* **C 50** (2007) 353 [hep-ph/0612161] [INSPIRE].

[51] CMS collaboration, *Identification and filtering of uncharacteristic noise in the CMS hadron calorimeter*, 2010 *JINST* **5** T03014 [arXiv:0911.4881] [INSPIRE].

[52] M. Cacciari, G.P. Salam and G. Soyez, *The anti-k_t jet clustering algorithm*, *JHEP* **04** (2008) 063 [arXiv:0802.1189] [INSPIRE].

[53] M. Cacciari, G.P. Salam and G. Soyez, *FastJet user manual*, *Eur. Phys. J.* **C 72** (2012) 1896 [arXiv:1111.6097] [INSPIRE].

[54] CMS collaboration, *Performance of CMS muon reconstruction in pp collision events at $\sqrt{s} = 7$ TeV*, 2012 *JINST* **7** P10002 [arXiv:1206.4071] [INSPIRE].

[55] CMS collaboration, G. Abbiendi, *The CMS muon system in Run2: preparation, status and first results*, PoS(EPS-HEP2015)237 [arXiv:1510.05424] [INSPIRE].

[56] P. Biallass and T. Hebbeker, *Parametrization of the cosmic muon flux for the generator CMSCGEN*, arXiv:0907.5514 [INSPIRE].

[57] D. Heck et al., *CORSIKA: A Monte Carlo code to simulate extensive air showers*, FZKA-6019 (1998).

[58] CMS collaboration, *Measurement of the charge ratio of atmospheric muons with the CMS detector*, *Phys. Lett.* **B 692** (2010) 83 [arXiv:1005.5332] [INSPIRE].

[59] CMS collaboration, *Measurements of inclusive W and Z cross sections in pp collisions at* $\sqrt{s} = 7$ *TeV*, *JHEP* **01** (2011) 080 [arXiv:1012.2466] [INSPIRE].

[60] M.J. Oreglia, *A study of the reactions* $\psi' \to \gamma\gamma\psi$, Ph.D. thesis, Stanford University, Stanford U.S.A. (1980).

[61] L. Landau, *On the energy loss of fast particles by ionization*, *J. Phys. (USSR)* **8** (1944) 201 [INSPIRE].

[62] CMS collaboration, *CMS luminosity measurement for the 2015 data-taking period*, CMS-PAS-LUM-15-001 (2015).

[63] CMS collaboration, *CMS luminosity measurements for the 2016 data taking period*, CMS-PAS-LUM-17-001 (2017).

[64] CMS collaboration, *Performance of the CMS Hadron Calorimeter with Cosmic Ray Muons and LHC Beam Data*, 2010 *JINST* **5** T03012 [arXiv:0911.4991] [INSPIRE].

[65] CMS collaboration, M. Schröder, *Performance of jets at CMS*, *J. Phys. Conf. Ser.* **587** (2015) 012004 [INSPIRE].

[66] T. Junk, *Confidence level computation for combining searches with small statistics*, *Nucl. Instrum. Meth.* **A 434** (1999) 435 [hep-ex/9902006] [INSPIRE].

[67] A.L. Read, *Presentation of search results: The CL(s) technique*, *J. Phys.* **G 28** (2002) 2693 [INSPIRE].

[68] R.D. Cousins and V.L. Highland, *Incorporating systematic uncertainties into an upper limit*, *Nucl. Instrum. Meth.* **A 320** (1992) 331 [INSPIRE].

The CMS collaboration

Yerevan Physics Institute, Yerevan, Armenia

A.M. Sirunyan, A. Tumasyan

Institut für Hochenergiephysik, Wien, Austria

W. Adam, F. Ambrogi, E. Asilar, T. Bergauer, J. Brandstetter, E. Brondolin, M. Dragicevic, J. Erö, A. Escalante Del Valle, M. Flechl, M. Friedl, R. Frühwirth[1], V.M. Ghete, J. Grossmann, J. Hrubec, M. Jeitler[1], A. König, N. Krammer, I. Krätschmer, D. Liko, T. Madlener, I. Mikulec, E. Pree, N. Rad, H. Rohringer, J. Schieck[1], R. Schöfbeck, M. Spanring, D. Spitzbart, A. Taurok, W. Waltenberger, J. Wittmann, C.-E. Wulz[1], M. Zarucki

Institute for Nuclear Problems, Minsk, Belarus

V. Chekhovsky, V. Mossolov, J. Suarez Gonzalez

Universiteit Antwerpen, Antwerpen, Belgium

E.A. De Wolf, D. Di Croce, X. Janssen, J. Lauwers, M. Pieters, M. Van De Klundert, H. Van Haevermaet, P. Van Mechelen, N. Van Remortel

Vrije Universiteit Brussel, Brussel, Belgium

S. Abu Zeid, F. Blekman, J. D'Hondt, I. De Bruyn, J. De Clercq, K. Deroover, G. Flouris, D. Lontkovskyi, S. Lowette, I. Marchesini, S. Moortgat, L. Moreels, Q. Python, K. Skovpen, S. Tavernier, W. Van Doninck, P. Van Mulders, I. Van Parijs

Université Libre de Bruxelles, Bruxelles, Belgium

D. Beghin, B. Bilin, H. Brun, B. Clerbaux, G. De Lentdecker, H. Delannoy, B. Dorney, G. Fasanella, L. Favart, R. Goldouzian, A. Grebenyuk, A.K. Kalsi, T. Lenzi, J. Luetic, T. Maerschalk, T. Seva, E. Starling, C. Vander Velde, P. Vanlaer, D. Vannerom, R. Yonamine, F. Zenoni

Ghent University, Ghent, Belgium

T. Cornelis, D. Dobur, A. Fagot, M. Gul, I. Khvastunov[2], D. Poyraz, C. Roskas, D. Trocino, M. Tytgat, W. Verbeke, M. Vit, N. Zaganidis

Université Catholique de Louvain, Louvain-la-Neuve, Belgium

H. Bakhshiansohi, O. Bondu, S. Brochet, G. Bruno, C. Caputo, A. Caudron, P. David, S. De Visscher, C. Delaere, M. Delcourt, B. Francois, A. Giammanco, G. Krintiras, V. Lemaitre, A. Magitteri, A. Mertens, M. Musich, K. Piotrzkowski, L. Quertenmont, A. Saggio, M. Vidal Marono, S. Wertz, J. Zobec

Centro Brasileiro de Pesquisas Fisicas, Rio de Janeiro, Brazil

W.L. Aldá Júnior, F.L. Alves, G.A. Alves, L. Brito, G. Correia Silva, C. Hensel, A. Moraes, M.E. Pol, P. Rebello Teles

Universidade do Estado do Rio de Janeiro, Rio de Janeiro, Brazil

E. Belchior Batista Das Chagas, W. Carvalho, J. Chinellato[3], E. Coelho, E.M. Da Costa, G.G. Da Silveira[4], D. De Jesus Damiao, S. Fonseca De Souza, L.M. Huertas

Guativa, H. Malbouisson, M. Melo De Almeida, C. Mora Herrera, L. Mundim, H. Nogima, L.J. Sanchez Rosas, A. Santoro, A. Sznajder, M. Thiel, E.J. Tonelli Manganote[3], F. Torres Da Silva De Araujo, A. Vilela Pereira

Universidade Estadual Paulista [a], Universidade Federal do ABC [b], São Paulo, Brazil

S. Ahuja[a], C.A. Bernardes[a], T.R. Fernandez Perez Tomei[a], E.M. Gregores[b], P.G. Mercadante[b], S.F. Novaes[a], Sandra S. Padula[a], D. Romero Abad[b], J.C. Ruiz Vargas[a]

Institute for Nuclear Research and Nuclear Energy, Bulgarian Academy of Sciences, Sofia, Bulgaria

A. Aleksandrov, R. Hadjiiska, P. Iaydjiev, A. Marinov, M. Misheva, M. Rodozov, M. Shopova, G. Sultanov

University of Sofia, Sofia, Bulgaria

A. Dimitrov, L. Litov, B. Pavlov, P. Petkov

Beihang University, Beijing, China

W. Fang[5], X. Gao[5], L. Yuan

Institute of High Energy Physics, Beijing, China

M. Ahmad, J.G. Bian, G.M. Chen, H.S. Chen, M. Chen, Y. Chen, C.H. Jiang, D. Leggat, H. Liao, Z. Liu, F. Romeo, S.M. Shaheen, A. Spiezia, J. Tao, C. Wang, Z. Wang, E. Yazgan, H. Zhang, J. Zhao

State Key Laboratory of Nuclear Physics and Technology, Peking University, Beijing, China

Y. Ban, G. Chen, J. Li, Q. Li, S. Liu, Y. Mao, S.J. Qian, D. Wang, Z. Xu

Tsinghua University, Beijing, China

Y. Wang

Universidad de Los Andes, Bogota, Colombia

C. Avila, A. Cabrera, L.F. Chaparro Sierra, C. Florez, C.F. González Hernández, J.D. Ruiz Alvarez, M.A. Segura Delgado

University of Split, Faculty of Electrical Engineering, Mechanical Engineering and Naval Architecture, Split, Croatia

B. Courbon, N. Godinovic, D. Lelas, I. Puljak, P.M. Ribeiro Cipriano, T. Sculac

University of Split, Faculty of Science, Split, Croatia

Z. Antunovic, M. Kovac

Institute Rudjer Boskovic, Zagreb, Croatia

V. Brigljevic, D. Ferencek, K. Kadija, B. Mesic, A. Starodumov[6], T. Susa

University of Cyprus, Nicosia, Cyprus

M.W. Ather, A. Attikis, G. Mavromanolakis, J. Mousa, C. Nicolaou, F. Ptochos, P.A. Razis, H. Rykaczewski

Charles University, Prague, Czech Republic

M. Finger[7], M. Finger Jr.[7]

Universidad San Francisco de Quito, Quito, Ecuador

E. Carrera Jarrin

Academy of Scientific Research and Technology of the Arab Republic of Egypt, Egyptian Network of High Energy Physics, Cairo, Egypt

A.A. Abdelalim[8,9], Y. Assran[10,11], S. Elgammal[11]

National Institute of Chemical Physics and Biophysics, Tallinn, Estonia

S. Bhowmik, R.K. Dewanjee, M. Kadastik, L. Perrini, M. Raidal, C. Veelken

Department of Physics, University of Helsinki, Helsinki, Finland

P. Eerola, H. Kirschenmann, J. Pekkanen, M. Voutilainen

Helsinki Institute of Physics, Helsinki, Finland

J. Havukainen, J.K. Heikkilä, T. Järvinen, V. Karimäki, R. Kinnunen, T. Lampén, K. Lassila-Perini, S. Laurila, S. Lehti, T. Lindén, P. Luukka, T. Mäenpää, H. Siikonen, E. Tuominen, J. Tuominiemi

Lappeenranta University of Technology, Lappeenranta, Finland

T. Tuuva

IRFU, CEA, Université Paris-Saclay, Gif-sur-Yvette, France

M. Besancon, F. Couderc, M. Dejardin, D. Denegri, J.L. Faure, F. Ferri, S. Ganjour, S. Ghosh, A. Givernaud, P. Gras, G. Hamel de Monchenault, P. Jarry, C. Leloup, E. Locci, M. Machet, J. Malcles, G. Negro, J. Rander, A. Rosowsky, M.Ö. Sahin, M. Titov

Laboratoire Leprince-Ringuet, Ecole polytechnique, CNRS/IN2P3, Université Paris-Saclay, Palaiseau, France

A. Abdulsalam[12], C. Amendola, I. Antropov, S. Baffioni, F. Beaudette, P. Busson, L. Cadamuro, C. Charlot, R. Granier de Cassagnac, M. Jo, I. Kucher, S. Lisniak, A. Lobanov, J. Martin Blanco, M. Nguyen, C. Ochando, G. Ortona, P. Paganini, P. Pigard, R. Salerno, J.B. Sauvan, Y. Sirois, A.G. Stahl Leiton, Y. Yilmaz, A. Zabi, A. Zghiche

Université de Strasbourg, CNRS, IPHC UMR 7178, F-67000 Strasbourg, France

J.-L. Agram[13], J. Andrea, D. Bloch, J.-M. Brom, M. Buttignol, E.C. Chabert, C. Collard, E. Conte[13], X. Coubez, F. Drouhin[13], J.-C. Fontaine[13], D. Gelé, U. Goerlach, M. Jansová, P. Juillot, A.-C. Le Bihan, N. Tonon, P. Van Hove

Centre de Calcul de l'Institut National de Physique Nucleaire et de Physique des Particules, CNRS/IN2P3, Villeurbanne, France

S. Gadrat

Université de Lyon, Université Claude Bernard Lyon 1, CNRS-IN2P3, Institut de Physique Nucléaire de Lyon, Villeurbanne, France

S. Beauceron, C. Bernet, G. Boudoul, N. Chanon, R. Chierici, D. Contardo, P. Depasse, H. El Mamouni, J. Fay, L. Finco, S. Gascon, M. Gouzevitch, G. Grenier, B. Ille, F. Lagarde, I.B. Laktineh, M. Lethuillier, L. Mirabito, A.L. Pequegnot, S. Perries, A. Popov[14], V. Sordini, M. Vander Donckt, S. Viret, S. Zhang

Georgian Technical University, Tbilisi, Georgia

A. Khvedelidze[7]

Tbilisi State University, Tbilisi, Georgia

D. Lomidze

RWTH Aachen University, I. Physikalisches Institut, Aachen, Germany

C. Autermann, L. Feld, M.K. Kiesel, K. Klein, M. Lipinski, M. Preuten, C. Schomakers, J. Schulz, M. Teroerde, B. Wittmer, V. Zhukov[14]

RWTH Aachen University, III. Physikalisches Institut A, Aachen, Germany

A. Albert, D. Duchardt, M. Endres, M. Erdmann, S. Erdweg, T. Esch, R. Fischer, A. Güth, T. Hebbeker, C. Heidemann, K. Hoepfner, S. Knutzen, M. Merschmeyer, A. Meyer, P. Millet, S. Mukherjee, T. Pook, M. Radziej, H. Reithler, M. Rieger, F. Scheuch, D. Teyssier, S. Thüer

RWTH Aachen University, III. Physikalisches Institut B, Aachen, Germany

G. Flügge, B. Kargoll, T. Kress, A. Künsken, T. Müller, A. Nehrkorn, A. Nowack, C. Pistone, O. Pooth, A. Stahl[15]

Deutsches Elektronen-Synchrotron, Hamburg, Germany

M. Aldaya Martin, T. Arndt, C. Asawatangtrakuldee, K. Beernaert, O. Behnke, U. Behrens, A. Bermúdez Martínez, A.A. Bin Anuar, K. Borras[16], V. Botta, A. Campbell, P. Connor, C. Contreras-Campana, F. Costanza, C. Diez Pardos, G. Eckerlin, D. Eckstein, T. Eichhorn, E. Eren, E. Gallo[17], J. Garay Garcia, A. Geiser, J.M. Grados Luyando, A. Grohsjean, P. Gunnellini, M. Guthoff, A. Harb, J. Hauk, M. Hempel[18], H. Jung, M. Kasemann, J. Keaveney, C. Kleinwort, I. Korol, D. Krücker, W. Lange, A. Lelek, T. Lenz, K. Lipka, W. Lohmann[18], R. Mankel, I.-A. Melzer-Pellmann, A.B. Meyer, M. Missiroli, G. Mittag, J. Mnich, A. Mussgiller, D. Pitzl, A. Raspereza, M. Savitskyi, P. Saxena, R. Shevchenko, N. Stefaniuk, H. Tholen, G.P. Van Onsem, R. Walsh, Y. Wen, K. Wichmann, C. Wissing, O. Zenaiev

University of Hamburg, Hamburg, Germany

R. Aggleton, S. Bein, V. Blobel, M. Centis Vignali, T. Dreyer, E. Garutti, D. Gonzalez, J. Haller, A. Hinzmann, M. Hoffmann, A. Karavdina, G. Kasieczka, R. Klanner, R. Kogler, N. Kovalchuk, S. Kurz, D. Marconi, M. Meyer, M. Niedziela, D. Nowatschin, T. Peiffer, A. Perieanu, C. Scharf, P. Schleper, A. Schmidt, S. Schumann, J. Schwandt, J. Sonneveld, H. Stadie, G. Steinbrück, F.M. Stober, M. Stöver, D. Troendle, E. Usai, A. Vanhoefer, B. Vormwald

Institut für Experimentelle Kernphysik, Karlsruhe, Germany

M. Akbiyik, C. Barth, M. Baselga, S. Baur, E. Butz, R. Caspart, T. Chwalek, F. Colombo, W. De Boer, A. Dierlamm, N. Faltermann, B. Freund, R. Friese, M. Giffels, M.A. Harrendorf, F. Hartmann[15], S.M. Heindl, U. Husemann, F. Kassel[15], S. Kudella, H. Mildner, M.U. Mozer, Th. Müller, M. Plagge, G. Quast, K. Rabbertz, M. Schröder, I. Shvetsov, G. Sieber, H.J. Simonis, R. Ulrich, S. Wayand, M. Weber, T. Weiler, S. Williamson, C. Wöhrmann, R. Wolf

Institute of Nuclear and Particle Physics (INPP), NCSR Demokritos, Aghia Paraskevi, Greece

G. Anagnostou, G. Daskalakis, T. Geralis, A. Kyriakis, D. Loukas, I. Topsis-Giotis

National and Kapodistrian University of Athens, Athens, Greece

G. Karathanasis, S. Kesisoglou, A. Panagiotou, N. Saoulidou, E. Tziaferi

National Technical University of Athens, Athens, Greece

K. Kousouris

University of Ioánnina, Ioánnina, Greece

I. Evangelou, C. Foudas, P. Gianneios, P. Katsoulis, P. Kokkas, S. Mallios, N. Manthos, I. Papadopoulos, E. Paradas, J. Strologas, F.A. Triantis, D. Tsitsonis

MTA-ELTE Lendület CMS Particle and Nuclear Physics Group, Eötvös Loránd University, Budapest, Hungary

M. Csanad, N. Filipovic, G. Pasztor, O. Surányi, G.I. Veres[19]

Wigner Research Centre for Physics, Budapest, Hungary

G. Bencze, C. Hajdu, D. Horvath[20], Á. Hunyadi, F. Sikler, V. Veszpremi, G. Vesztergombi[19]

Institute of Nuclear Research ATOMKI, Debrecen, Hungary

N. Beni, S. Czellar, J. Karancsi[21], A. Makovec, J. Molnar, Z. Szillasi

Institute of Physics, University of Debrecen, Debrecen, Hungary

M. Bartók[19], P. Raics, Z.L. Trocsanyi, B. Ujvari

Indian Institute of Science (IISc), Bangalore, India

S. Choudhury, J.R. Komaragiri

National Institute of Science Education and Research, Bhubaneswar, India

S. Bahinipati[22], P. Mal, K. Mandal, A. Nayak[23], D.K. Sahoo[22], N. Sahoo, S.K. Swain

Panjab University, Chandigarh, India

S. Bansal, S.B. Beri, V. Bhatnagar, R. Chawla, N. Dhingra, A. Kaur, M. Kaur, S. Kaur, R. Kumar, P. Kumari, A. Mehta, J.B. Singh, G. Walia

University of Delhi, Delhi, India

Ashok Kumar, Aashaq Shah, A. Bhardwaj, S. Chauhan, B.C. Choudhary, R.B. Garg, S. Keshri, A. Kumar, S. Malhotra, M. Naimuddin, K. Ranjan, R. Sharma

Saha Institute of Nuclear Physics, HBNI, Kolkata, India

R. Bhardwaj[24], R. Bhattacharya, S. Bhattacharya, U. Bhawandeep[24], D. Bhowmik, S. Dey, S. Dutt[24], S. Dutta, S. Ghosh, N. Majumdar, A. Modak, K. Mondal, S. Mukhopadhyay, S. Nandan, A. Purohit, P.K. Rout, A. Roy, S. Roy Chowdhury, S. Sarkar, M. Sharan, B. Singh, S. Thakur[24]

Indian Institute of Technology Madras, Madras, India

P.K. Behera

Bhabha Atomic Research Centre, Mumbai, India

R. Chudasama, D. Dutta, V. Jha, V. Kumar, A.K. Mohanty[15], P.K. Netrakanti, L.M. Pant, P. Shukla, A. Topkar

Tata Institute of Fundamental Research-A, Mumbai, India

T. Aziz, S. Dugad, B. Mahakud, S. Mitra, G.B. Mohanty, N. Sur, B. Sutar

Tata Institute of Fundamental Research-B, Mumbai, India

S. Banerjee, S. Bhattacharya, S. Chatterjee, P. Das, M. Guchait, Sa. Jain, S. Kumar, M. Maity[25], G. Majumder, K. Mazumdar, T. Sarkar[25], N. Wickramage[26]

Indian Institute of Science Education and Research (IISER), Pune, India

S. Chauhan, S. Dube, V. Hegde, A. Kapoor, K. Kothekar, S. Pandey, A. Rane, S. Sharma

Institute for Research in Fundamental Sciences (IPM), Tehran, Iran

S. Chenarani[27], E. Eskandari Tadavani, S.M. Etesami[27], M. Khakzad, M. Mohammadi Najafabadi, M. Naseri, S. Paktinat Mehdiabadi[28], F. Rezaei Hosseinabadi, B. Safarzadeh[29], M. Zeinali

University College Dublin, Dublin, Ireland

M. Felcini, M. Grunewald

INFN Sezione di Bari [a], Università di Bari [b], Politecnico di Bari [c], Bari, Italy

M. Abbrescia[a,b], C. Calabria[a,b], A. Colaleo[a], D. Creanza[a,c], L. Cristella[a,b], N. De Filippis[a,c], M. De Palma[a,b], A. Di Florio[a,b], F. Errico[a,b], L. Fiore[a], G. Iaselli[a,c], S. Lezki[a,b], G. Maggi[a,c], M. Maggi[a], B. Marangelli[a,b], G. Miniello[a,b], S. My[a,b], S. Nuzzo[a,b], A. Pompili[a,b], G. Pugliese[a,c], R. Radogna[a], A. Ranieri[a], G. Selvaggi[a,b], A. Sharma[a], L. Silvestris[a,15], R. Venditti[a], P. Verwilligen[a], G. Zito[a]

INFN Sezione di Bologna [a], Università di Bologna [b], Bologna, Italy

G. Abbiendi[a], C. Battilana[a,b], D. Bonacorsi[a,b], L. Borgonovi[a,b], S. Braibant-Giacomelli[a,b], R. Campanini[a,b], P. Capiluppi[a,b], A. Castro[a,b], F.R. Cavallo[a], S.S. Chhibra[a,b], G. Codispoti[a,b], M. Cuffiani[a,b], G.M. Dallavalle[a], F. Fabbri[a], A. Fanfani[a,b], D. Fasanella[a,b], P. Giacomelli[a], C. Grandi[a], L. Guiducci[a,b], F. Iemmi, S. Marcellini[a], G. Masetti[a], A. Montanari[a], F.L. Navarria[a,b], A. Perrotta[a], A.M. Rossi[a,b], T. Rovelli[a,b], G.P. Siroli[a,b], N. Tosi[a]

INFN Sezione di Catania [a], Università di Catania [b], Catania, Italy

S. Albergo[a,b], S. Costa[a,b], A. Di Mattia[a], F. Giordano[a,b], R. Potenza[a,b], A. Tricomi[a,b], C. Tuve[a,b]

INFN Sezione di Firenze ^{a}**, Università di Firenze** ^{b}**, Firenze, Italy**

G. Barbagli^a, K. Chatterjee^{a,b}, V. Ciulli^{a,b}, C. Civinini^a, R. D'Alessandro^{a,b}, E. Focardi^{a,b}, G. Latino, P. Lenzi^{a,b}, M. Meschini^a, S. Paoletti^a, L. Russo^{a,30}, G. Sguazzoni^a, D. Strom^a, L. Viliani^a

INFN Laboratori Nazionali di Frascati, Frascati, Italy

L. Benussi, S. Bianco, F. Fabbri, D. Piccolo, F. Primavera^{15}

INFN Sezione di Genova ^{a}**, Università di Genova** ^{b}**, Genova, Italy**

V. Calvelli^{a,b}, F. Ferro^a, F. Ravera^{a,b}, E. Robutti^a, S. Tosi^{a,b}

INFN Sezione di Milano-Bicocca ^{a}**, Università di Milano-Bicocca** ^{b}**, Milano, Italy**

A. Benaglia^a, A. Beschi^b, L. Brianza^{a,b}, F. Brivio^{a,b}, V. Ciriolo^{a,b,15}, M.E. Dinardo^{a,b}, S. Fiorendi^{a,b}, S. Gennai^a, A. Ghezzi^{a,b}, P. Govoni^{a,b}, M. Malberti^{a,b}, S. Malvezzi^a, R.A. Manzoni^{a,b}, D. Menasce^a, L. Moroni^a, M. Paganoni^{a,b}, K. Pauwels^{a,b}, D. Pedrini^a, S. Pigazzini^{a,b,31}, S. Ragazzi^{a,b}, T. Tabarelli de Fatis^{a,b}

INFN Sezione di Napoli ^{a}**, Università di Napoli 'Federico II'** ^{b}**, Napoli, Italy, Università della Basilicata** ^{c}**, Potenza, Italy, Università G. Marconi** ^{d}**, Roma, Italy**

S. Buontempo^a, N. Cavallo^{a,c}, S. Di Guida^{a,d,15}, F. Fabozzi^{a,c}, F. Fienga^{a,b}, A.O.M. Iorio^{a,b}, W.A. Khan^a, L. Lista^a, S. Meola^{a,d,15}, P. Paolucci^{a,15}, C. Sciacca^{a,b}, F. Thyssen^a

INFN Sezione di Padova ^{a}**, Università di Padova** ^{b}**, Padova, Italy, Università di Trento** ^{c}**, Trento, Italy**

P. Azzi^a, N. Bacchetta^a, L. Benato^{a,b}, D. Bisello^{a,b}, A. Boletti^{a,b}, R. Carlin^{a,b}, A. Carvalho Antunes De Oliveira^{a,b}, P. Checchia^a, M. Dall'Osso^{a,b}, P. De Castro Manzano^a, T. Dorigo^a, U. Dosselli^a, U. Gasparini^{a,b}, A. Gozzelino^a, S. Lacaprara^a, P. Lujan, M. Margoni^{a,b}, A.T. Meneguzzo^{a,b}, N. Pozzobon^{a,b}, P. Ronchese^{a,b}, R. Rossin^{a,b}, F. Simonetto^{a,b}, A. Tiko, E. Torassa^a, M. Zanetti^{a,b}, P. Zotto^{a,b}, G. Zumerle^{a,b}

INFN Sezione di Pavia ^{a}**, Università di Pavia** ^{b}**, Pavia, Italy**

A. Braghieri^a, A. Magnani^a, P. Montagna^{a,b}, S.P. Ratti^{a,b}, V. Re^a, M. Ressegotti^{a,b}, C. Riccardi^{a,b}, P. Salvini^a, I. Vai^{a,b}, P. Vitulo^{a,b}

INFN Sezione di Perugia ^{a}**, Università di Perugia** ^{b}**, Perugia, Italy**

L. Alunni Solestizi^{a,b}, M. Biasini^{a,b}, G.M. Bilei^a, C. Cecchi^{a,b}, D. Ciangottini^{a,b}, L. Fanò^{a,b}, P. Lariccia^{a,b}, R. Leonardi^{a,b}, E. Manoni^a, G. Mantovani^{a,b}, V. Mariani^{a,b}, M. Menichelli^a, A. Rossi^{a,b}, A. Santocchia^{a,b}, D. Spiga^a

INFN Sezione di Pisa ^{a}**, Università di Pisa** ^{b}**, Scuola Normale Superiore di Pisa** ^{c}**, Pisa, Italy**

K. Androsov^a, P. Azzurri^{a,15}, G. Bagliesi^a, L. Bianchini^a, T. Boccali^a, L. Borrello, R. Castaldi^a, M.A. Ciocci^{a,b}, R. Dell'Orso^a, G. Fedi^a, L. Giannini^{a,c}, A. Giassi^a, M.T. Grippo^{a,30}, F. Ligabue^{a,c}, T. Lomtadze^a, E. Manca^{a,c}, G. Mandorli^{a,c},

A. Messineo^{a,b}, F. Palla^a, A. Rizzi^{a,b}, P. Spagnolo^a, R. Tenchini^a, G. Tonelli^{a,b}, A. Venturi^a, P.G. Verdini^a

INFN Sezione di Roma ^{a}, **Sapienza Università di Roma** ^{b}, **Rome, Italy**

L. Barone^{a,b}, F. Cavallari^a, M. Cipriani^{a,b}, N. Daci^a, D. Del Re^{a,b}, E. Di Marco^{a,b}, M. Diemoz^a, S. Gelli^{a,b}, E. Longo^{a,b}, F. Margaroli^{a,b}, B. Marzocchi^{a,b}, P. Meridiani^a, G. Organtini^{a,b}, R. Paramatti^{a,b}, F. Preiato^{a,b}, S. Rahatlou^{a,b}, C. Rovelli^a, F. Santanastasio^{a,b}

INFN Sezione di Torino ^{a}, **Università di Torino** ^{b}, **Torino, Italy, Università del Piemonte Orientale** ^{c}, **Novara, Italy**

N. Amapane^{a,b}, R. Arcidiacono^{a,c}, S. Argiro^{a,b}, M. Arneodo^{a,c}, N. Bartosik^a, R. Bellan^{a,b}, C. Biino^a, N. Cartiglia^a, R. Castello^{a,b}, F. Cenna^{a,b}, M. Costa^{a,b}, R. Covarelli^{a,b}, A. Degano^{a,b}, N. Demaria^a, B. Kiani^{a,b}, C. Mariotti^a, S. Maselli^a, E. Migliore^{a,b}, V. Monaco^{a,b}, E. Monteil^{a,b}, M. Monteno^a, M.M. Obertino^{a,b}, L. Pacher^{a,b}, N. Pastrone^a, M. Pelliccioni^a, G.L. Pinna Angioni^{a,b}, A. Romero^{a,b}, M. Ruspa^{a,c}, R. Sacchi^{a,b}, K. Shchelina^{a,b}, V. Sola^a, A. Solano^{a,b}, A. Staiano^a, P. Traczyk^{a,b}

INFN Sezione di Trieste ^{a}, **Università di Trieste** ^{b}, **Trieste, Italy**

S. Belforte^a, M. Casarsa^a, F. Cossutti^a, G. Della Ricca^{a,b}, A. Zanetti^a

Kyungpook National University, Daegu, Korea

D.H. Kim, G.N. Kim, M.S. Kim, J. Lee, S. Lee, S.W. Lee, C.S. Moon, Y.D. Oh, S. Sekmen, D.C. Son, Y.C. Yang

Chonnam National University, Institute for Universe and Elementary Particles, Kwangju, Korea

H. Kim, D.H. Moon, G. Oh

Hanyang University, Seoul, Korea

J.A. Brochero Cifuentes, J. Goh, T.J. Kim

Korea University, Seoul, Korea

S. Cho, S. Choi, Y. Go, D. Gyun, S. Ha, B. Hong, Y. Jo, Y. Kim, K. Lee, K.S. Lee, S. Lee, J. Lim, S.K. Park, Y. Roh

Seoul National University, Seoul, Korea

J. Almond, J. Kim, J.S. Kim, H. Lee, K. Lee, K. Nam, S.B. Oh, B.C. Radburn-Smith, S.h. Seo, U.K. Yang, H.D. Yoo, G.B. Yu

University of Seoul, Seoul, Korea

H. Kim, J.H. Kim, J.S.H. Lee, I.C. Park

Sungkyunkwan University, Suwon, Korea

Y. Choi, C. Hwang, J. Lee, I. Yu

Vilnius University, Vilnius, Lithuania

V. Dudenas, A. Juodagalvis, J. Vaitkus

National Centre for Particle Physics, Universiti Malaya, Kuala Lumpur, Malaysia

I. Ahmed, Z.A. Ibrahim, M.A.B. Md Ali[32], F. Mohamad Idris[33], W.A.T. Wan Abdullah, M.N. Yusli, Z. Zolkapli

Centro de Investigacion y de Estudios Avanzados del IPN, Mexico City, Mexico

Reyes-Almanza, R, Ramirez-Sanchez, G., Duran-Osuna, M. C., H. Castilla-Valdez, E. De La Cruz-Burelo, I. Heredia-De La Cruz[34], Rabadan-Trejo, R. I., R. Lopez-Fernandez, J. Mejia Guisao, A. Sanchez-Hernandez

Universidad Iberoamericana, Mexico City, Mexico

S. Carrillo Moreno, C. Oropeza Barrera, F. Vazquez Valencia

Benemerita Universidad Autonoma de Puebla, Puebla, Mexico

J. Eysermans, I. Pedraza, H.A. Salazar Ibarguen, C. Uribe Estrada

Universidad Autónoma de San Luis Potosí, San Luis Potosí, Mexico

A. Morelos Pineda

University of Auckland, Auckland, New Zealand

D. Krofcheck

University of Canterbury, Christchurch, New Zealand

P.H. Butler

National Centre for Physics, Quaid-I-Azam University, Islamabad, Pakistan

A. Ahmad, M. Ahmad, Q. Hassan, H.R. Hoorani, A. Saddique, M.A. Shah, M. Shoaib, M. Waqas

National Centre for Nuclear Research, Swierk, Poland

H. Bialkowska, M. Bluj, B. Boimska, T. Frueboes, M. Górski, M. Kazana, K. Nawrocki, M. Szleper, P. Zalewski

Institute of Experimental Physics, Faculty of Physics, University of Warsaw, Warsaw, Poland

K. Bunkowski, A. Byszuk[35], K. Doroba, A. Kalinowski, M. Konecki, J. Krolikowski, M. Misiura, M. Olszewski, A. Pyskir, M. Walczak

Laboratório de Instrumentação e Física Experimental de Partículas, Lisboa, Portugal

P. Bargassa, C. Beirão Da Cruz E Silva, A. Di Francesco, P. Faccioli, B. Galinhas, M. Gallinaro, J. Hollar, N. Leonardo, L. Lloret Iglesias, M.V. Nemallapudi, J. Seixas, G. Strong, O. Toldaiev, D. Vadruccio, J. Varela

Joint Institute for Nuclear Research, Dubna, Russia

S. Afanasiev, P. Bunin, M. Gavrilenko, I. Golutvin, I. Gorbunov, A. Kamenev, V. Karjavin, A. Lanev, A. Malakhov, V. Matveev[36,37], P. Moisenz, V. Palichik, V. Perelygin, S. Shmatov, S. Shulha, N. Skatchkov, V. Smirnov, N. Voytishin, A. Zarubin

Petersburg Nuclear Physics Institute, Gatchina (St. Petersburg), Russia

Y. Ivanov, V. Kim[38], E. Kuznetsova[39], P. Levchenko, V. Murzin, V. Oreshkin, I. Smirnov, D. Sosnov, V. Sulimov, L. Uvarov, S. Vavilov, A. Vorobyev

Institute for Nuclear Research, Moscow, Russia

Yu. Andreev, A. Dermenev, S. Gninenko, N. Golubev, A. Karneyeu, M. Kirsanov, N. Krasnikov, A. Pashenkov, D. Tlisov, A. Toropin

Institute for Theoretical and Experimental Physics, Moscow, Russia

V. Epshteyn, V. Gavrilov, N. Lychkovskaya, V. Popov, I. Pozdnyakov, G. Safronov, A. Spiridonov, A. Stepennov, V. Stolin, M. Toms, E. Vlasov, A. Zhokin

Moscow Institute of Physics and Technology, Moscow, Russia

T. Aushev, A. Bylinkin[37]

National Research Nuclear University 'Moscow Engineering Physics Institute' (MEPhI), Moscow, Russia

R. Chistov[40], M. Danilov[40], P. Parygin, D. Philippov, S. Polikarpov, E. Tarkovskii

P.N. Lebedev Physical Institute, Moscow, Russia

V. Andreev, M. Azarkin[37], I. Dremin[37], M. Kirakosyan[37], S.V. Rusakov, A. Terkulov

Skobeltsyn Institute of Nuclear Physics, Lomonosov Moscow State University, Moscow, Russia

A. Baskakov, A. Belyaev, E. Boos, M. Dubinin[41], L. Dudko, A. Ershov, A. Gribushin, V. Klyukhin, O. Kodolova, I. Lokhtin, I. Miagkov, S. Obraztsov, S. Petrushanko, V. Savrin, A. Snigirev

Novosibirsk State University (NSU), Novosibirsk, Russia

V. Blinov[42], D. Shtol[42], Y. Skovpen[42]

State Research Center of Russian Federation, Institute for High Energy Physics of NRC "Kurchatov Institute", Protvino, Russia

I. Azhgirey, I. Bayshev, S. Bitioukov, D. Elumakhov, A. Godizov, V. Kachanov, A. Kalinin, D. Konstantinov, P. Mandrik, V. Petrov, R. Ryutin, A. Sobol, S. Troshin, N. Tyurin, A. Uzunian, A. Volkov

National Research Tomsk Polytechnic University, Tomsk, Russia

A. Babaev

University of Belgrade, Faculty of Physics and Vinca Institute of Nuclear Sciences, Belgrade, Serbia

P. Adzic[43], P. Cirkovic, D. Devetak, M. Dordevic, J. Milosevic

Centro de Investigaciones Energéticas Medioambientales y Tecnológicas (CIEMAT), Madrid, Spain

J. Alcaraz Maestre, I. Bachiller, M. Barrio Luna, M. Cerrada, N. Colino, B. De La Cruz, A. Delgado Peris, C. Fernandez Bedoya, J.P. Fernández Ramos, J. Flix, M.C. Fouz, O. Gonzalez Lopez, S. Goy Lopez, J.M. Hernandez, M.I. Josa, D. Moran, A. Pérez-Calero

Yzquierdo, J. Puerta Pelayo, I. Redondo, L. Romero, M.S. Soares, A. Triossi, A. Álvarez Fernández

Universidad Autónoma de Madrid, Madrid, Spain

C. Albajar, J.F. de Trocóniz

Universidad de Oviedo, Oviedo, Spain

J. Cuevas, C. Erice, J. Fernandez Menendez, S. Folgueras, I. Gonzalez Caballero, J.R. González Fernández, E. Palencia Cortezon, S. Sanchez Cruz, P. Vischia, J.M. Vizan Garcia

Instituto de Física de Cantabria (IFCA), CSIC-Universidad de Cantabria, Santander, Spain

I.J. Cabrillo, A. Calderon, B. Chazin Quero, J. Duarte Campderros, M. Fernandez, P.J. Fernández Manteca, J. Garcia-Ferrero, A. García Alonso, G. Gomez, A. Lopez Virto, J. Marco, C. Martinez Rivero, P. Martinez Ruiz del Arbol, F. Matorras, J. Piedra Gomez, C. Prieels, T. Rodrigo, A. Ruiz-Jimeno, L. Scodellaro, N. Trevisani, I. Vila, R. Vilar Cortabitarte

CERN, European Organization for Nuclear Research, Geneva, Switzerland

D. Abbaneo, B. Akgun, E. Auffray, P. Baillon, A.H. Ball, D. Barney, J. Bendavid, M. Bianco, A. Bocci, C. Botta, T. Camporesi, M. Cepeda, G. Cerminara, E. Chapon, Y. Chen, D. d'Enterria, A. Dabrowski, V. Daponte, A. David, M. De Gruttola, A. De Roeck, N. Deelen, M. Dobson, T. du Pree, M. Dünser, N. Dupont, A. Elliott-Peisert, P. Everaerts, F. Fallavollita[44], G. Franzoni, J. Fulcher, W. Funk, D. Gigi, A. Gilbert, K. Gill, F. Glege, D. Gulhan, J. Hegeman, V. Innocente, A. Jafari, P. Janot, O. Karacheban[18], J. Kieseler, V. Knünz, A. Kornmayer, M.J. Kortelainen, M. Krammer[1], C. Lange, P. Lecoq, C. Lourenço, M.T. Lucchini, L. Malgeri, M. Mannelli, A. Martelli, F. Meijers, J.A. Merlin, S. Mersi, E. Meschi, P. Milenovic[45], F. Moortgat, M. Mulders, H. Neugebauer, J. Ngadiuba, S. Orfanelli, L. Orsini, F. Pantaleo[15], L. Pape, E. Perez, M. Peruzzi, A. Petrilli, G. Petrucciani, A. Pfeiffer, M. Pierini, F.M. Pitters, D. Rabady, A. Racz, T. Reis, G. Rolandi[46], M. Rovere, H. Sakulin, C. Schäfer, C. Schwick, M. Seidel, M. Selvaggi, A. Sharma, P. Silva, P. Sphicas[47], A. Stakia, J. Steggemann, M. Stoye, M. Tosi, D. Treille, A. Tsirou, V. Veckalns[48], M. Verweij, W.D. Zeuner

Paul Scherrer Institut, Villigen, Switzerland

W. Bertl[†], L. Caminada[49], K. Deiters, W. Erdmann, R. Horisberger, Q. Ingram, H.C. Kaestli, D. Kotlinski, U. Langenegger, T. Rohe, S.A. Wiederkehr

ETH Zurich — Institute for Particle Physics and Astrophysics (IPA), Zurich, Switzerland

M. Backhaus, L. Bäni, P. Berger, B. Casal, G. Dissertori, M. Dittmar, M. Donegà, C. Dorfer, C. Grab, C. Heidegger, D. Hits, J. Hoss, T. Klijnsma, W. Lustermann, B. Mangano, M. Marionneau, M.T. Meinhard, D. Meister, F. Micheli, P. Musella, F. Nessi-Tedaldi, F. Pandolfi, J. Pata, F. Pauss, G. Perrin, L. Perrozzi, M. Quittnat, M. Reichmann,

D.A. Sanz Becerra, M. Schönenberger, L. Shchutska, V.R. Tavolaro, K. Theofilatos, M.L. Vesterbacka Olsson, R. Wallny, D.H. Zhu

Universität Zürich, Zurich, Switzerland

T.K. Aarrestad, C. Amsler[50], D. Brzhechko, M.F. Canelli, A. De Cosa, R. Del Burgo, S. Donato, C. Galloni, T. Hreus, B. Kilminster, I. Neutelings, D. Pinna, G. Rauco, P. Robmann, D. Salerno, K. Schweiger, C. Seitz, Y. Takahashi, A. Zucchetta

National Central University, Chung-Li, Taiwan

V. Candelise, Y.H. Chang, K.y. Cheng, T.H. Doan, Sh. Jain, R. Khurana, C.M. Kuo, W. Lin, A. Pozdnyakov, S.S. Yu

National Taiwan University (NTU), Taipei, Taiwan

Arun Kumar, P. Chang, Y. Chao, K.F. Chen, P.H. Chen, F. Fiori, W.-S. Hou, Y. Hsiung, Y.F. Liu, R.-S. Lu, E. Paganis, A. Psallidas, A. Steen, J.f. Tsai

Chulalongkorn University, Faculty of Science, Department of Physics, Bangkok, Thailand

B. Asavapibhop, K. Kovitanggoon, G. Singh, N. Srimanobhas

Çukurova University, Physics Department, Science and Art Faculty, Adana, Turkey

A. Bat, F. Boran, S. Cerci[51], S. Damarseckin, Z.S. Demiroglu, C. Dozen, I. Dumanoglu, S. Girgis, G. Gokbulut, Y. Guler, I. Hos[52], E.E. Kangal[53], O. Kara, A. Kayis Topaksu, U. Kiminsu, M. Oglakci, G. Onengut, K. Ozdemir[54], D. Sunar Cerci[51], B. Tali[51], U.G. Tok, S. Turkcapar, I.S. Zorbakir, C. Zorbilmez

Middle East Technical University, Physics Department, Ankara, Turkey

G. Karapinar[55], K. Ocalan[56], M. Yalvac, M. Zeyrek

Bogazici University, Istanbul, Turkey

E. Gülmez, M. Kaya[57], O. Kaya[58], S. Tekten, E.A. Yetkin[59]

Istanbul Technical University, Istanbul, Turkey

M.N. Agaras, S. Atay, A. Cakir, K. Cankocak, Y. Komurcu

Institute for Scintillation Materials of National Academy of Science of Ukraine, Kharkov, Ukraine

B. Grynyov

National Scientific Center, Kharkov Institute of Physics and Technology, Kharkov, Ukraine

L. Levchuk

University of Bristol, Bristol, United Kingdom

F. Ball, L. Beck, J.J. Brooke, D. Burns, E. Clement, D. Cussans, O. Davignon, H. Flacher, J. Goldstein, G.P. Heath, H.F. Heath, L. Kreczko, D.M. Newbold[60], S. Paramesvaran, T. Sakuma, S. Seif El Nasr-storey, D. Smith, V.J. Smith

Rutherford Appleton Laboratory, Didcot, United Kingdom

K.W. Bell, A. Belyaev[61], C. Brew, R.M. Brown, L. Calligaris, D. Cieri, D.J.A. Cockerill, J.A. Coughlan, K. Harder, S. Harper, J. Linacre, E. Olaiya, D. Petyt, C.H. Shepherd-Themistocleous, A. Thea, I.R. Tomalin, T. Williams, W.J. Womersley

Imperial College, London, United Kingdom

G. Auzinger, R. Bainbridge, P. Bloch, J. Borg, S. Breeze, O. Buchmuller, A. Bundock, S. Casasso, D. Colling, L. Corpe, P. Dauncey, G. Davies, M. Della Negra, R. Di Maria, Y. Haddad, G. Hall, G. Iles, T. James, M. Komm, R. Lane, C. Laner, L. Lyons, A.-M. Magnan, S. Malik, L. Mastrolorenzo, T. Matsushita, J. Nash[62], A. Nikitenko[6], V. Palladino, M. Pesaresi, A. Richards, A. Rose, E. Scott, C. Seez, A. Shtipliyski, T. Strebler, S. Summers, A. Tapper, K. Uchida, M. Vazquez Acosta[63], T. Virdee[15], N. Wardle, D. Winterbottom, J. Wright, S.C. Zenz

Brunel University, Uxbridge, United Kingdom

J.E. Cole, P.R. Hobson, A. Khan, P. Kyberd, A. Morton, I.D. Reid, L. Teodorescu, S. Zahid

Baylor University, Waco, U.S.A.

A. Borzou, K. Call, J. Dittmann, K. Hatakeyama, H. Liu, N. Pastika, C. Smith

Catholic University of America, Washington DC, U.S.A.

R. Bartek, A. Dominguez

The University of Alabama, Tuscaloosa, U.S.A.

A. Buccilli, S.I. Cooper, C. Henderson, P. Rumerio, C. West

Boston University, Boston, U.S.A.

D. Arcaro, A. Avetisyan, T. Bose, D. Gastler, D. Rankin, C. Richardson, J. Rohlf, L. Sulak, D. Zou

Brown University, Providence, U.S.A.

G. Benelli, D. Cutts, M. Hadley, J. Hakala, U. Heintz, J.M. Hogan[64], K.H.M. Kwok, E. Laird, G. Landsberg, J. Lee, Z. Mao, M. Narain, J. Pazzini, S. Piperov, S. Sagir, R. Syarif, D. Yu

University of California, Davis, Davis, U.S.A.

R. Band, C. Brainerd, R. Breedon, D. Burns, M. Calderon De La Barca Sanchez, M. Chertok, J. Conway, R. Conway, P.T. Cox, R. Erbacher, C. Flores, G. Funk, W. Ko, R. Lander, C. Mclean, M. Mulhearn, D. Pellett, J. Pilot, S. Shalhout, M. Shi, J. Smith, D. Stolp, D. Taylor, K. Tos, M. Tripathi, Z. Wang, F. Zhang

University of California, Los Angeles, U.S.A.

M. Bachtis, C. Bravo, R. Cousins, A. Dasgupta, A. Florent, J. Hauser, M. Ignatenko, N. Mccoll, S. Regnard, D. Saltzberg, C. Schnaible, V. Valuev

University of California, Riverside, Riverside, U.S.A.

E. Bouvier, K. Burt, R. Clare, J. Ellison, J.W. Gary, S.M.A. Ghiasi Shirazi, G. Hanson, G. Karapostoli, E. Kennedy, F. Lacroix, O.R. Long, M. Olmedo Negrete, M.I. Paneva, W. Si, L. Wang, H. Wei, S. Wimpenny, B. R. Yates

University of California, San Diego, La Jolla, U.S.A.

J.G. Branson, S. Cittolin, M. Derdzinski, R. Gerosa, D. Gilbert, B. Hashemi, A. Holzner, D. Klein, G. Kole, V. Krutelyov, J. Letts, M. Masciovecchio, D. Olivito, S. Padhi, M. Pieri, M. Sani, V. Sharma, S. Simon, M. Tadel, A. Vartak, S. Wasserbaech[65], J. Wood, F. Würthwein, A. Yagil, G. Zevi Della Porta

University of California, Santa Barbara — Department of Physics, Santa Barbara, U.S.A.

N. Amin, R. Bhandari, J. Bradmiller-Feld, C. Campagnari, M. Citron, A. Dishaw, V. Dutta, M. Franco Sevilla, L. Gouskos, R. Heller, J. Incandela, A. Ovcharova, H. Qu, J. Richman, D. Stuart, I. Suarez, J. Yoo

California Institute of Technology, Pasadena, U.S.A.

D. Anderson, A. Bornheim, J. Bunn, J.M. Lawhorn, H.B. Newman, T. Q. Nguyen, C. Pena, M. Spiropulu, J.R. Vlimant, R. Wilkinson, S. Xie, Z. Zhang, R.Y. Zhu

Carnegie Mellon University, Pittsburgh, U.S.A.

M.B. Andrews, T. Ferguson, T. Mudholkar, M. Paulini, J. Russ, M. Sun, H. Vogel, I. Vorobiev, M. Weinberg

University of Colorado Boulder, Boulder, U.S.A.

J.P. Cumalat, W.T. Ford, F. Jensen, A. Johnson, M. Krohn, S. Leontsinis, E. Macdonald, T. Mulholland, K. Stenson, K.A. Ulmer, S.R. Wagner

Cornell University, Ithaca, U.S.A.

J. Alexander, J. Chaves, Y. Cheng, J. Chu, A. Datta, S. Dittmer, K. Mcdermott, N. Mirman, J.R. Patterson, D. Quach, A. Rinkevicius, A. Ryd, L. Skinnari, L. Soffi, S.M. Tan, Z. Tao, J. Thom, J. Tucker, P. Wittich, M. Zientek

Fermi National Accelerator Laboratory, Batavia, U.S.A.

S. Abdullin, M. Albrow, M. Alyari, G. Apollinari, A. Apresyan, A. Apyan, S. Banerjee, L.A.T. Bauerdick, A. Beretvas, J. Berryhill, P.C. Bhat, G. Bolla[†], K. Burkett, J.N. Butler, A. Canepa, G.B. Cerati, H.W.K. Cheung, F. Chlebana, M. Cremonesi, J. Duarte, V.D. Elvira, J. Freeman, Z. Gecse, E. Gottschalk, L. Gray, D. Green, S. Grünendahl, O. Gutsche, J. Hanlon, R.M. Harris, S. Hasegawa, J. Hirschauer, Z. Hu, B. Jayatilaka, S. Jindariani, M. Johnson, U. Joshi, B. Klima, B. Kreis, S. Lammel, D. Lincoln, R. Lipton, M. Liu, T. Liu, R. Lopes De Sá, J. Lykken, K. Maeshima, N. Magini, J.M. Marraffino, D. Mason, P. McBride, P. Merkel, S. Mrenna, S. Nahn, V. O'Dell, K. Pedro, O. Prokofyev, G. Rakness, L. Ristori, A. Savoy-Navarro[66], B. Schneider, E. Sexton-Kennedy, A. Soha, W.J. Spalding, L. Spiegel, S. Stoynev, J. Strait, N. Strobbe, L. Taylor, S. Tkaczyk, N.V. Tran, L. Uplegger, E.W. Vaandering, C. Vernieri, M. Verzocchi, R. Vidal, M. Wang, H.A. Weber, A. Whitbeck, W. Wu

University of Florida, Gainesville, U.S.A.

D. Acosta, P. Avery, P. Bortignon, D. Bourilkov, A. Brinkerhoff, A. Carnes, M. Carver, D. Curry, R.D. Field, I.K. Furic, S.V. Gleyzer, B.M. Joshi, J. Konigsberg, A. Korytov,

K. Kotov, P. Ma, K. Matchev, H. Mei, G. Mitselmakher, K. Shi, D. Sperka, N. Terentyev, L. Thomas, J. Wang, S. Wang, J. Yelton

Florida International University, Miami, U.S.A.

Y.R. Joshi, S. Linn, P. Markowitz, J.L. Rodriguez

Florida State University, Tallahassee, U.S.A.

A. Ackert, T. Adams, A. Askew, S. Hagopian, V. Hagopian, K.F. Johnson, T. Kolberg, G. Martinez, T. Perry, H. Prosper, A. Saha, A. Santra, V. Sharma, R. Yohay

Florida Institute of Technology, Melbourne, U.S.A.

M.M. Baarmand, V. Bhopatkar, S. Colafranceschi, M. Hohlmann, D. Noonan, T. Roy, F. Yumiceva

University of Illinois at Chicago (UIC), Chicago, U.S.A.

M.R. Adams, L. Apanasevich, D. Berry, R.R. Betts, R. Cavanaugh, X. Chen, O. Evdokimov, C.E. Gerber, D.A. Hangal, D.J. Hofman, K. Jung, J. Kamin, I.D. Sandoval Gonzalez, M.B. Tonjes, N. Varelas, H. Wang, Z. Wu, J. Zhang

The University of Iowa, Iowa City, U.S.A.

B. Bilki[67], W. Clarida, K. Dilsiz[68], S. Durgut, R.P. Gandrajula, M. Haytmyradov, V. Khristenko, J.-P. Merlo, H. Mermerkaya[69], A. Mestvirishvili, A. Moeller, J. Nachtman, H. Ogul[70], Y. Onel, F. Ozok[71], A. Penzo, C. Snyder, E. Tiras, J. Wetzel, K. Yi

Johns Hopkins University, Baltimore, U.S.A.

B. Blumenfeld, A. Cocoros, N. Eminizer, D. Fehling, L. Feng, A.V. Gritsan, P. Maksimovic, J. Roskes, U. Sarica, M. Swartz, M. Xiao, C. You

The University of Kansas, Lawrence, U.S.A.

A. Al-bataineh, P. Baringer, A. Bean, S. Boren, J. Bowen, J. Castle, S. Khalil, A. Kropivnitskaya, D. Majumder, W. Mcbrayer, M. Murray, C. Rogan, C. Royon, S. Sanders, E. Schmitz, J.D. Tapia Takaki, Q. Wang

Kansas State University, Manhattan, U.S.A.

A. Ivanov, K. Kaadze, Y. Maravin, A. Mohammadi, L.K. Saini, N. Skhirtladze

Lawrence Livermore National Laboratory, Livermore, U.S.A.

F. Rebassoo, D. Wright

University of Maryland, College Park, U.S.A.

A. Baden, O. Baron, A. Belloni, S.C. Eno, Y. Feng, C. Ferraioli, N.J. Hadley, S. Jabeen, G.Y. Jeng, R.G. Kellogg, J. Kunkle, A.C. Mignerey, F. Ricci-Tam, Y.H. Shin, A. Skuja, S.C. Tonwar

Massachusetts Institute of Technology, Cambridge, U.S.A.

D. Abercrombie, B. Allen, V. Azzolini, R. Barbieri, A. Baty, G. Bauer, R. Bi, S. Brandt, W. Busza, I.A. Cali, M. D'Alfonso, Z. Demiragli, G. Gomez Ceballos, M. Goncharov, P. Harris, D. Hsu, M. Hu, Y. Iiyama, G.M. Innocenti, M. Klute, D. Kovalskyi, Y.-J. Lee, A. Levin, P.D. Luckey, B. Maier, A.C. Marini, C. Mcginn, C. Mironov, S. Narayanan,

X. Niu, C. Paus, C. Roland, G. Roland, J. Salfeld-Nebgen, G.S.F. Stephans, K. Sumorok, K. Tatar, D. Velicanu, J. Wang, T.W. Wang, B. Wyslouch

University of Minnesota, Minneapolis, U.S.A.

A.C. Benvenuti, R.M. Chatterjee, A. Evans, P. Hansen, S. Kalafut, Y. Kubota, Z. Lesko, J. Mans, S. Nourbakhsh, N. Ruckstuhl, R. Rusack, J. Turkewitz, M.A. Wadud

University of Mississippi, Oxford, U.S.A.

J.G. Acosta, S. Oliveros

University of Nebraska-Lincoln, Lincoln, U.S.A.

E. Avdeeva, K. Bloom, D.R. Claes, C. Fangmeier, F. Golf, R. Gonzalez Suarez, R. Kamalieddin, I. Kravchenko, J. Monroy, J.E. Siado, G.R. Snow, B. Stieger

State University of New York at Buffalo, Buffalo, U.S.A.

J. Dolen, A. Godshalk, C. Harrington, I. Iashvili, D. Nguyen, A. Parker, S. Rappoccio, B. Roozbahani

Northeastern University, Boston, U.S.A.

G. Alverson, E. Barberis, C. Freer, A. Hortiangtham, A. Massironi, D.M. Morse, T. Orimoto, R. Teixeira De Lima, T. Wamorkar, B. Wang, A. Wisecarver, D. Wood

Northwestern University, Evanston, U.S.A.

S. Bhattacharya, O. Charaf, K.A. Hahn, N. Mucia, N. Odell, M.H. Schmitt, K. Sung, M. Trovato, M. Velasco

University of Notre Dame, Notre Dame, U.S.A.

R. Bucci, N. Dev, M. Hildreth, K. Hurtado Anampa, C. Jessop, D.J. Karmgard, N. Kellams, K. Lannon, W. Li, N. Loukas, N. Marinelli, F. Meng, C. Mueller, Y. Musienko[36], M. Planer, A. Reinsvold, R. Ruchti, P. Siddireddy, G. Smith, S. Taroni, M. Wayne, A. Wightman, M. Wolf, A. Woodard

The Ohio State University, Columbus, U.S.A.

J. Alimena, L. Antonelli, B. Bylsma, L.S. Durkin, S. Flowers, B. Francis, A. Hart, C. Hill, W. Ji, T.Y. Ling, W. Luo, B.L. Winer, H.W. Wulsin

Princeton University, Princeton, U.S.A.

S. Cooperstein, O. Driga, P. Elmer, J. Hardenbrook, P. Hebda, S. Higginbotham, A. Kalogeropoulos, D. Lange, J. Luo, D. Marlow, K. Mei, I. Ojalvo, J. Olsen, C. Palmer, P. Piroué, D. Stickland, C. Tully

University of Puerto Rico, Mayaguez, U.S.A.

S. Malik, S. Norberg

Purdue University, West Lafayette, U.S.A.

A. Barker, V.E. Barnes, S. Das, L. Gutay, M. Jones, A.W. Jung, A. Khatiwada, D.H. Miller, N. Neumeister, C.C. Peng, H. Qiu, J.F. Schulte, J. Sun, F. Wang, R. Xiao, W. Xie

Purdue University Northwest, Hammond, U.S.A.

T. Cheng, N. Parashar

Rice University, Houston, U.S.A.

Z. Chen, K.M. Ecklund, S. Freed, F.J.M. Geurts, M. Guilbaud, M. Kilpatrick, W. Li, B. Michlin, B.P. Padley, J. Roberts, J. Rorie, W. Shi, Z. Tu, J. Zabel, A. Zhang

University of Rochester, Rochester, U.S.A.

A. Bodek, P. de Barbaro, R. Demina, Y.t. Duh, T. Ferbel, M. Galanti, A. Garcia-Bellido, J. Han, O. Hindrichs, A. Khukhunaishvili, K.H. Lo, P. Tan, M. Verzetti

The Rockefeller University, New York, U.S.A.

R. Ciesielski, K. Goulianos, C. Mesropian

Rutgers, The State University of New Jersey, Piscataway, U.S.A.

A. Agapitos, J.P. Chou, Y. Gershtein, T.A. Gómez Espinosa, E. Halkiadakis, M. Heindl, E. Hughes, S. Kaplan, R. Kunnawalkam Elayavalli, S. Kyriacou, A. Lath, R. Montalvo, K. Nash, M. Osherson, H. Saka, S. Salur, S. Schnetzer, D. Sheffield, S. Somalwar, R. Stone, S. Thomas, P. Thomassen, M. Walker

University of Tennessee, Knoxville, U.S.A.

A.G. Delannoy, J. Heideman, G. Riley, K. Rose, S. Spanier, K. Thapa

Texas A&M University, College Station, U.S.A.

O. Bouhali[72], A. Castaneda Hernandez[72], A. Celik, M. Dalchenko, M. De Mattia, A. Delgado, S. Dildick, R. Eusebi, J. Gilmore, T. Huang, T. Kamon[73], R. Mueller, Y. Pakhotin, R. Patel, A. Perloff, L. Perniè, D. Rathjens, A. Safonov, A. Tatarinov

Texas Tech University, Lubbock, U.S.A.

N. Akchurin, J. Damgov, F. De Guio, P.R. Dudero, J. Faulkner, E. Gurpinar, S. Kunori, K. Lamichhane, S.W. Lee, T. Mengke, S. Muthumuni, T. Peltola, S. Undleeb, I. Volobouev, Z. Wang

Vanderbilt University, Nashville, U.S.A.

S. Greene, A. Gurrola, R. Janjam, W. Johns, C. Maguire, A. Melo, H. Ni, K. Padeken, P. Sheldon, S. Tuo, J. Velkovska, Q. Xu

University of Virginia, Charlottesville, U.S.A.

M.W. Arenton, P. Barria, B. Cox, R. Hirosky, M. Joyce, A. Ledovskoy, H. Li, C. Neu, T. Sinthuprasith, Y. Wang, E. Wolfe, F. Xia

Wayne State University, Detroit, U.S.A.

R. Harr, P.E. Karchin, N. Poudyal, J. Sturdy, P. Thapa, S. Zaleski

University of Wisconsin — Madison, Madison, WI, U.S.A.

M. Brodski, J. Buchanan, C. Caillol, D. Carlsmith, S. Dasu, L. Dodd, S. Duric, B. Gomber, M. Grothe, M. Herndon, A. Hervé, U. Hussain, P. Klabbers, A. Lanaro, A. Levine, K. Long, R. Loveless, V. Rekovic, T. Ruggles, A. Savin, N. Smith, W.H. Smith, N. Woods

†: Deceased
1: Also at Vienna University of Technology, Vienna, Austria
2: Also at IRFU, CEA, Université Paris-Saclay, Gif-sur-Yvette, France
3: Also at Universidade Estadual de Campinas, Campinas, Brazil

4: Also at Federal University of Rio Grande do Sul, Porto Alegre, Brazil

5: Also at Université Libre de Bruxelles, Bruxelles, Belgium

6: Also at Institute for Theoretical and Experimental Physics, Moscow, Russia

7: Also at Joint Institute for Nuclear Research, Dubna, Russia

8: Also at Helwan University, Cairo, Egypt

9: Now at Zewail City of Science and Technology, Zewail, Egypt

10: Also at Suez University, Suez, Egypt

11: Now at British University in Egypt, Cairo, Egypt

12: Also at Department of Physics, King Abdulaziz University, Jeddah, Saudi Arabia

13: Also at Université de Haute Alsace, Mulhouse, France

14: Also at Skobeltsyn Institute of Nuclear Physics, Lomonosov Moscow State University, Moscow, Russia

15: Also at CERN, European Organization for Nuclear Research, Geneva, Switzerland

16: Also at RWTH Aachen University, III. Physikalisches Institut A, Aachen, Germany

17: Also at University of Hamburg, Hamburg, Germany

18: Also at Brandenburg University of Technology, Cottbus, Germany

19: Also at MTA-ELTE Lendület CMS Particle and Nuclear Physics Group, Eötvös Loránd University, Budapest, Hungary

20: Also at Institute of Nuclear Research ATOMKI, Debrecen, Hungary

21: Also at Institute of Physics, University of Debrecen, Debrecen, Hungary

22: Also at Indian Institute of Technology Bhubaneswar, Bhubaneswar, India

23: Also at Institute of Physics, Bhubaneswar, India

24: Also at Shoolini University, Solan, India

25: Also at University of Visva-Bharati, Santiniketan, India

26: Also at University of Ruhuna, Matara, Sri Lanka

27: Also at Isfahan University of Technology, Isfahan, Iran

28: Also at Yazd University, Yazd, Iran

29: Also at Plasma Physics Research Center, Science and Research Branch, Islamic Azad University, Tehran, Iran

30: Also at Università degli Studi di Siena, Siena, Italy

31: Also at INFN Sezione di Milano-Bicocca; Università di Milano-Bicocca, Milano, Italy

32: Also at International Islamic University of Malaysia, Kuala Lumpur, Malaysia

33: Also at Malaysian Nuclear Agency, MOSTI, Kajang, Malaysia

34: Also at Consejo Nacional de Ciencia y Tecnología, Mexico city, Mexico

35: Also at Warsaw University of Technology, Institute of Electronic Systems, Warsaw, Poland

36: Also at Institute for Nuclear Research, Moscow, Russia

37: Now at National Research Nuclear University 'Moscow Engineering Physics Institute' (MEPhI), Moscow, Russia

38: Also at St. Petersburg State Polytechnical University, St. Petersburg, Russia

39: Also at University of Florida, Gainesville, U.S.A.

40: Also at P.N. Lebedev Physical Institute, Moscow, Russia

41: Also at California Institute of Technology, Pasadena, U.S.A.

42: Also at Budker Institute of Nuclear Physics, Novosibirsk, Russia

43: Also at Faculty of Physics, University of Belgrade, Belgrade, Serbia

44: Also at INFN Sezione di Pavia; Università di Pavia, Pavia, Italy

45: Also at University of Belgrade, Faculty of Physics and Vinca Institute of Nuclear Sciences, Belgrade, Serbia

46: Also at Scuola Normale e Sezione dell'INFN, Pisa, Italy

47: Also at National and Kapodistrian University of Athens, Athens, Greece

48: Also at Riga Technical University, Riga, Latvia

49: Also at Universität Zürich, Zurich, Switzerland

50: Also at Stefan Meyer Institute for Subatomic Physics (SMI), Vienna, Austria

51: Also at Adiyaman University, Adiyaman, Turkey

52: Also at Istanbul Aydin University, Istanbul, Turkey

53: Also at Mersin University, Mersin, Turkey

54: Also at Piri Reis University, Istanbul, Turkey

55: Also at Izmir Institute of Technology, Izmir, Turkey

56: Also at Necmettin Erbakan University, Konya, Turkey

57: Also at Marmara University, Istanbul, Turkey

58: Also at Kafkas University, Kars, Turkey

59: Also at Istanbul Bilgi University, Istanbul, Turkey

60: Also at Rutherford Appleton Laboratory, Didcot, United Kingdom

61: Also at School of Physics and Astronomy, University of Southampton, Southampton, United Kingdom

62: Also at Monash University, Faculty of Science, Clayton, Australia

63: Also at Instituto de Astrofísica de Canarias, La Laguna, Spain

64: Also at Bethel University, ST. PAUL, U.S.A.

65: Also at Utah Valley University, Orem, U.S.A.

66: Also at Purdue University, West Lafayette, U.S.A.

67: Also at Beykent University, Istanbul, Turkey

68: Also at Bingol University, Bingol, Turkey

69: Also at Erzincan University, Erzincan, Turkey

70: Also at Sinop University, Sinop, Turkey

71: Also at Mimar Sinan University, Istanbul, Istanbul, Turkey

72: Also at Texas A&M University at Qatar, Doha, Qatar

73: Also at Kyungpook National University, Daegu, Korea